PNAS
www.pnas.org

Supplementary Information for

A Comparative Genomics Approach Identifies Contact-Dependent Growth Inhibition as a Virulence Determinant

Jonathan P. Allen, Egon A. Ozer, George Minasov, Ludmilla Shuvalova, Olga Kiryukhina, Karla J. F. Satchell, and Alan R. Hauser

Jonathan P. Allen
Email: jallen19@luc.edu

This PDF file includes:

www.pnas.org/cgi/doi/10.1073/pnas.1919198117

Materials and Methods

Genomic analyses. A core genome of *P. aeruginosa* was defined using SPINE(1) based on the complete genomic sequences of 12 reference strains: 19BR, 213BR, B136-33, DK2, LESB58, M18, NCGM2.S1, PA7, PACS2, PAO1, RP73 and PA14. A sequence was allowed to be missing from up to one of these twelve genomes and still be considered core. AGEnt was then used to determine the accessory genome sequences of each of the 100 PABL isolates by subtracting the core genome from its whole genome(1). ClustAGE was used to determine patterns of shared accessory sequence among different isolates(2). ClustAGE searches through the multitude of genomic fragments from the accessory genome of every isolate and aligns them to the longest shared contiguous accessory sequence available. This collection of shared accessory sequence is referred to as a "bin" with the longest representative sequence referred to as the "bin representative". In this way the pool of accessory genomic sequence is organized into bins of shared sequences. Bins were then further processed into subelements based upon alignment breakpoints so that patterns of common contiguous accessory sequence could be analyzed for their presence or absence among the PABL isolates. Subelement presence or absence was correlated with virulence ranking using the Spearman correlation test in R. Only subelements greater than or equal to 100bp in length were investigated. Amino acid sequences of open reading frames (ORFs) within the subelements were screened against the MvirDB database (http://mvirdb.llnl.gov/) using BLAST. Only BLAST hits with bitscores greater than or equal to 90 were considered positive hits. ORFs were also screened using EffectiveDB (https://effectors.csb.univie.ac.at) to determine the presence of putative type III secretion signals, Sec secretion signals, or regions with eukaryotic homology. If subelements passing these filters were located adjacent to each other in highly virulent strains, such subelements were merged together as a single virulence-associated accessory genomic element (AGEv). Alternatively, if the subelement was the only genetic unit passing these filters then the subelement itself was referred to as an AGEv.

To determine the genetic context of each AGEv, sequences flanking the AGEv were used as query for BLAST analysis against all complete *P. aeruginosa* genome sequences in NCBI.

AGEv were often portions of larger mobile genetic elements; thus, BLAST results were used to determine shared genetic borders between isolates containing the aforementioned mobile element and reference isolates that did not. Sequences were extracted, annotated when necessary using BASYS(3) and manually refined using Artemis(4). Certain sequences were analyzed for phage genes using PHASTER (http://phaster.ca)(5). The genetic context of the AGEv was visualized compared to a reference strain using EasyFig(6).

Cloning and strain construction. The plasmid pJA001 was first constructed as a template for PCR amplification of a gentamicin resistance cassette flanked by FRT sites to use in the generation of *P. aeruginosa* mutants by allelic exchange. To construct pJA001, the miniCTX1 plasmid(7) was used as template for PCR amplification of a 4,765 kb backbone fragment with primers oligo161 and oligo162. This fragment contained the tetracycline resistance gene, a pMB1-derived origin of replication, an integrase enzyme, and FRT sites but excluded the *attP* phage attachment site as well as the multiple cloning site. The gentamicin-resistance cassette from pEX18.GM was PCR amplified using oligo163 and oligo164. Each fragment was digested with BamHI and EcoRI and ligated with T4 DNA ligase (NEB) to generate pJA001. This final vector construct was used as a PCR template to amplify the FRT-flanked gentamicin-resistance cassette (FRT:gm) using oligo165 and oligo166 for subsequent cloning steps.

P. aeruginosa chromosomal deletions were generated using the procedure of Schweizer and colleagues(8). Cloning vectors were designed to generate allelic replacement constructs in which (1) the target chromosomal region would be replaced with the FRT:gm cassette described above, (2) an unmarked in-frame deletion of the target chromosomal region would be created, or (3) an unmarked in-frame deletion would be repaired by reintroducing an intact copy of the deleted gene at its native site. For cloning strategy 1, plasmids pJA004 through pJA032 were constructed for allelic replacement of AGEvs and AGExs with a gentamicin-resistance cassette (Table S2). Forward (F) and Reverse (R) primers were used to PCR amplify ~500 nucleotides of homologous sequence flanking the upstream (up) or downstream (dn) regions of the respective AGEv targets. Primer pairs homologous to the upstream and downstream regions were referred to as Fup/Rup

and Fdn/Rdn respectively (Table S3). For example, PCR amplification of the upstream and downstream regions flanking AGEv1 used the primer pairs oligo2/oligo4 and oligo1/oligo3 respectively (Table S3). Corresponding upstream and downstream PCR fragments were combined with the FRT:gm PCR fragment (discussed above) via splicing by overhang extension (SOE) PCR to generate a final cloning fragment in which the FRT:gm was flanked by the homologous sequences of the gene to be replaced. Complete fragments were gel isolated, digested and ligated into either the XbaI or XmaI restriction site of pEX18.AP(8). In the example above, the oligo2/4 and oligo1/3 PCR fragments would be combined by SOE-PCR using oligo2 and oligo3, and this combined product would be ligated into the cut pEX18.AP to generate pJA004 (Table S2). For cloning strategy 2, plasmids pJA039 through pJA041 and pJA047 were constructed for generating clean deletion mutants in *P. aeruginosa* (Table S2). Plasmids were assembled similar to the process used above except the 500 nucleotide PCR fragments flanking the deletion target were combined using Gibson assembly into the EcoRI site of pEX18-GM without the FRT:gm PCR fragment. For cloning strategy 3, plasmids pJA039 through pJA042 and pJA043 were constructed to repair *cdiA* mutations in *P. aeruginosa* (Table S2). Primers were designed to amplify the previously deleted genetic target plus 500bp of flanking sequence. This fragment was gel purified and inserted into the EcoRI site of pEX18-GM by Gibson assembly.

Deletion vectors were either transformed into *P. aeruginosa* isolates by electroporation(9) or introduced by conjugation using S17.1 *E. coli*(10, 11). Merodiploids were isolated on antibiotic supplemented media and subsequently resolved by sucrose counter-selection. Final constructs were screened by replica plating for antibiotic susceptibility and confirmed by PCR and sequencing of the amplified fragment. To resolve the FRT:gm cassette, mutants were transformed with pFLP2 by electroporation and selection on LB-carb plates. Colonies were subsequently purged of the pFLP2 vector by sucrose selection and screened by replica plating on LB, LB-carb, and LB-gm. All final mutant strains were confirmed by whole genome sequencing on an Illumina MiSeq instrument (Miseq Reagent Kit V3, 600-cycle, Illumina).

The plasmid pJPA1 was generated for use as an arabinose-inducible expression vector in *P. aeruginosa*. The *araBAD* promoter (pBAD) was PCR amplified from pTKRED using primers

oligo167 and oligo168. This fragment was then cloned into the KpnI/HindIII fragment of pFLP2 to generate pJPA1. pJPA1 contains a broad-host-range origin of replication, an ampicillin resistance marker, the counterselectable *sacB* marker, an *oriT* for conjugation-mediated plasmid transfer and an engineered multiple cloning site under transcriptional control of the *araBAD* promoter. The plasmid pJA002 was then generated to express *cdi1I*^{PABL017} in pJPA1 for episomal expression of the immunity gene. *cdi1I*^{PABL017} was amplified from genomic DNA using primers oligo169 and oligo170 and cloned into pJPA1 digested with XbaI and KpnI. For chromosomal expression of *cdi1I*^{PABL017} under arabinose induction, the entire pBAD_Cdi1I^{PABL017} cassette was PCR amplified from pJA002 using primers oligo171 and oligo172 and cloned into the HindIII site of miniCTX1 to generate pJA003. Introduction of pJA003 into the *attB* site of *P. aeruginosa* was performed as previously described(7).

The plasmids pJA035 and pJA036 were generated for expression and in-vitro purification of two different Cdi1A-CT^{PABL017} constructs beginning at the corresponding Cdi1A^{PABL017} amino acids 3108 and 3345 respectively. Each construct included the Cdi1A-CT^{PABL017} sequence along with the downstream *cdiI* immunity gene, which was amplified using primer pairs oligo159/158 and oligo155/158 respectively. Target amplicons were cloned into the SspI site of the bacterial expression vector pMCSG53 by Gibson assembly. This resulted in a final expressed product containing an N-terminal 6X-His tag with an internal Tobacco Etch Virus (TEV) Protease cleavage site(12). The plasmid pJA037 was generated similarly to pJA036 except that the sequence was altered such that the Cdi1A^{PABL017} catalytic residue His3372 was substituted with an alanine. To generate the H3372A substitution, two separate PCR fragments were amplified using oligo155 and oligo174, and oligo173 and oligo156. These two fragments were then cloned into pMCSG53 by Gibson assembly as described. Finally, pJA049 was designed to express Cdi1I^{PABL017} with a C-terminal terminal Strep-tag II(13) for separate purification and detection. The gene was PCR amplified from pJA045 using primers oligo157 and oligo160 and cloned into the NdeI/SspI site of pMCSG53. This removes the N-terminal 6xHIS tag but retains the T7 promoter. All expression constructs were introduced into BL21(DE3) *E. coli* and expression was verified by Western blot

analysis using either an α-6xHis antibody (Takara) or α-Strep-tag II antibody (Abcam) following isopropyl β-D-1-thiogalactopranoside (IPTG) induction.

The plasmids pJA044, pJA045 and pJA046 were generated for expression of CdiA-CT^{PABL017}, CdiA-CT^{PABL017} [H3372A], or CdiI^{PABL017} within transfected eukaryotic cells. The plasmid pEF1α-IRES-AcGFP1A (Clontech) was used as the backbone cloning vector. This vector allows for the constitutive expression of cloned targets by the EF1α promoter. GFP production from an internal ribosomal entry site (IRES) on the bicistronic transcript allows identification of transfected cells. All targets were PCR amplified using the corresponding primers listed in Table S2 and cloned into the EcoRI site of pEF1α-IRES-AcGFP1A by Gibson Assembly. Plasmids were maintained in Top10 *E. coli* for purification and use in transfection studies.

Transposon mutagenesis analysis. Genomic DNA from the stored transposon mutant pool was isolated using a Maxwell® 16 Processor (Promega) with the Maxwell® 16 Cell DNA Purification Kit per manufacturer instructions. Identification of transposon insertion sites was accomplished by Illumina sequencing of semi-random PCR products as follows. Primers oligo175 and oligo176 were used for the first semi-random PCR amplification step of the pooled transposon mutant DNA under the following conditions: 94˚C for 3 minutes, followed by 10 cycles of 94˚C for 20 seconds, 50˚C for 40 seconds and 72˚C for 3 minutes, and 25 cycles of 94˚C for 30 seconds, 62˚C for 40 seconds and 72˚C for 3 minutes. Products were PCR purified using the QIAquick PCR purification kit (Qiagen). Round 1 PCR products were used as template for a second round of amplification using oligo177 and oligo178 under the following conditions: 94˚C for 3 minutes followed by 34 cycles of 94˚C for 30 seconds, 57˚C for 40 seconds and 72˚C for 1 minute with a final extension of 72˚C for 5 minutes. PCR products were purified as before and used in a final round of amplification to add adapter sequences with oligo179 and oligo180 required for the subsequent Illumina indexing reaction. Cycling conditions were 94˚C for 3 minutes followed by 30 cycles of 94˚C for 30 seconds, 57˚C for 40 seconds and 72˚C for 1 minute with a final 5-minute extension at 72˚C. Products were PCR purified as before and quantified by fluorometric analysis (Invitrogen Quant-iT™ dsDNA Assay

Kit, High Sensitivity). The purified PCR products were indexed and prepared for sequencing on an Illumina MiSeq instrument (Miseq Reagent Kit V3, 600-cycle, Illumina).

To identify transposon insertion sites, raw Illumina reads were first trimmed for low quality or N bases using the Trimmomatic paired end script(14) with a 4-base sliding window, average quality score limit of 20 and overall minimum read length of 250. The following Bash scripts were then used to filter reads that contain either (1) the core transposon sequence or (2) the core sequence from the universal *P. aeruginosa* primer (oligo175): (Script 1) zcat TnSeq_R1.fq.gz | paste - - - - | awk -v FS="\t" -v OFS="\n" '$2 ~ "AGACCGGGGACTTATCAGCCAACCTGTTA" {print $1, $2, $3, $4}' | gzip > TnSeq_R1_filtered.fq.gz; (Script 2) zcat TnSeq_R2.fq.gz | paste - - - - | awk -v FS="\t" -v OFS="\n" '$2 ~ "GGCCACGCGTCGACTAGTAG.....CAGCAG" {print $1, $2, $3, $4}' | gzip > TnSeq_R2_filtered.fq.gz. The filtered fastq.gz files were unzipped and resynchronized using fastq-pair (https://github.com/linsalrob/fastq-pair). Transposon and primer sequences from the resynchronized paired-end reads were removed using the program Cutadapt. The filtered Fastq files were converted to fasta format using the Qiime1 convert_fastaqual_fastq.py script(15). Reads with at least 90% identity were then identified and quantified using the Qiime1 scripts pick_otus.py and pick_rep_set.py respectively. Finally, the location of these reads within the PABL017 genome was determined using BLAST(16).

Protein expression and purification. For in vitro enzymatic assays, purification of Cdi1A-CT^{PABL017} was performed under denaturing conditions to separate the enzymatic CT from the immunity protein. Briefly, *E. coli* strains expressing 6xHis tagged protein constructs were subcultured from overnight growth in 1 L of LB-amp to an OD_{600} of ~0.6. IPTG was added to a final concentration of 1 mM to induce expression, and the culture was grown for an additional 4 hr. Cells were chilled on ice and pelleted by centrifugation at 4 ˚C for 20 min at 11,000 x *g*. Cell pellets were resuspended in 100 ml cold native extraction buffer (20 mM sodium phosphate [pH 7.0], 200 mM sodium chloride, 10 mM β-mercaptoethanol, 1 mM phenylmethylsulfonyl fluoride) and sonicated on ice using a Q500 Sonicator (QSonica) affixed with a CL-334 probe and 12 mm microtip under the following conditions: 20 cycles of a 10 second, 60% amplitude pulse with a 50 second pause.

Lysates were cleared by centrifugation at 4 ˚C for 20 min at 11,000 x *g*. Supernatants were passed through a 0.2 µm polyethersulfone filter (Fisher Scientific), mixed with Ni-nitrilotriacetic acid superflow resin (Qiagen) for 30 min and centrifuged in a hanging bucket rotor for 10 min at 1000 x *g*. The supernatants were carefully aspirated and the resin pellet was suspended in 10 ml of denaturing buffer (20 mM sodium phosphate [pH 7.0], 200 mM sodium chloride, 10 mM β-mercaptoethanol, 6M guanidine HCl). The resin mix was loaded onto a Poly-Prep column (Bio-Rad) and allowed to settle for 20 min. The column was washed with 10 ml of denaturing buffer followed by 150 ml of native wash buffer (20 mM sodium phosphate [pH 7.0], 200 mM sodium chloride, 15 mM imidazole, 10 mM β-mercaptoethanol). Proteins were eluted from the column in four 1-ml-fractions of native elution buffer (20 mM sodium phosphate [pH 7.0], 200 mM sodium chloride, 200 mM imidazole). Proteins were dialyzed at 4˚C overnight in native storage buffer (20 mM sodium phosphate (pH 7.0), 200 mM sodium chloride), and concentrated using a Spin-X® UF 6 concentrator (Sigma) at a 10,000 molecular weight cutoff. *E. coli* strains expressing *Strep*-tag II fusion protein constructs were cultured and pelleted as described above. Cell pellets were suspended in 50 ml of buffer W (100 mM Tris-HCl [pH 8.0], 150 mM sodium chloride, 1 mM ethylenediaminetetraacetic acid [EDTA]), and sonicated as above. Clarified lysates were loaded onto a Strep-Tactin® Sepharose® (IBA Life Sciences) prepared column and washed with 25 mL of buffer W. Proteins were eluted from the column in five-1-ml-fractions of buffer E (100 mM Tris/HCl [pH 8.0], 150 mM sodium chloride, 1 mM EDTA, 2.5 mM desthiobiotin). Proteins were dialyzed at 4˚C overnight in 100 mM Tris/HCl [pH 8.0], 150 mM sodium chloride, and concentrated as above.

For purification of the CdiA-CT^{PABL017} + CdiI complex for crystallization, *E. coli* BL21 (DE3) cells (Invitrogen) transformed with pJPA035 were grown at 37˚C and 220 rev min^{-1} in 4 liters of M9 Se-Met medium until the OD600 nm reached 0.2, at which time they were placed at 4˚C overnight. Growth at 37ºC was resumed the next morning and protein expression was induced with 0.6 mM IPTG when an OD600 nm of 1.6 was reached. The protein was expressed overnight with the shaking reduced to 200 rev min^{-1} and the temperature reduced to 22˚C. The cells were harvested by centrifugation as described previously (17). The resulting cell pellet was resuspended in 120 ml lysis buffer (0.5 M Arginine, 10 mM Tris–HCl [pH 8.3], 500 mM NaCl, 1 mM Tris [2-carboxyethyl]

phosphine, 10% glycerol, 0.01% IGEPAL CA-630, EDTA-free protease inhibitors [Roche; one tablet per 100 ml of buffer]) and the suspension was frozen at 20˚C until purification. The frozen suspension was thawed under cold running water, sonicated and centrifuged. The protein was purified in two steps using nickel (II) affinity chromatography (IMAC) followed by size-exclusion chromatography (SEC) as described previously(18) with modification. The concentration of NaCl in the low-imidazole buffer was increased to 1.0 M to reduce nonspecific binding. The polyhistidine tag was cleaved by incubation of the tagged protein with recombinant TEV protease overnight at 20ºC. The resulting protein was collected from the flow through with loading buffer containing 20 mM and 40 mM Imidazole. The purity of the protein was assessed by SDS–PAGE followed by Bio-Safe Coomassie G-250 staining (Bio-Rad).

Crystallization. Crystallization screening was setup at the protein concentration of 6.4 mg ml^{-1} in 10 mM Tris-HCl (pH 8.3), 5 mM BME in the presence or absence of 500 mM NaCl. Two microliter crystallization drops in 1:1 (protein : reservoir solution) ratio were equilibrated against 96 conditions per screen using commercially available Classics II, PACT, PEG's II and JCSG+ Suites (Qiagen). Diffraction quality crystals grew from 100 mM Bis-Tris (pH 5.5), 25% (w/v) PEG 3350 (Classics II Suite condition D6) and protein solution with 500 mM NaCl (Table S5).

Data collection and processing. Prior to flash-cooling in liquid nitrogen, crystals were transferred into a 5 µl drop of reservoir solution, which served as a cryoprotectant. Data were collected on the LS-CAT 21-ID-F beamline at the Advanced Photon Source (APS) at Argonne National Laboratory. A total of 300 images, which corresponded to 180 degrees of the spindle axis rotation were indexed, integrated and scaled using HKL-3000(19). Data collection and data processing statistics are listed in Table S6.

Structure solution and refinement. The structure of Cdi1A-$CT^{PABL017}$ in complex with CdiI was solved by Single Anomalous Dispersion (SAD) using HKL-3000 suite. The initial solution went through several rounds of refinement in REFMAC v.5.8(20) and manual model corrections using

Coot(21) from the CCP4 suite(22). Water molecules were generated using ARP/wARP (23). Translation–Libration–Screw (TLS) groups were created by the *TLSMD* server(24) (http://skuldbmsc.washington.edu/~tlsmd/) and TLS corrections were applied during the final stages of refinement. *MolProbity*(25) (http://molprobity.biochem.duke.edu/) was used for monitoring the quality of the model during refinement and for the final validation of the structure. The final model and diffraction data were deposited in the Protein Data Bank (https://www.rcsb.org/) with the assigned PDB code 6d7y. The final model consists of two polypeptide chains: chain A, which is the CT domain of Cdi1A (amino acids 3352 – 3443) and chain B, which is the immunity protein (amino acids 1–155). There are 98 water molecules in the crystal structure. Refinement statistics and the quality of the final model are summarized in Table S7. The structure of Cdi1A-CT^{PABL017} was compared against other 3D protein structures using DALI(26).

Northern blot analysis. CdiA-CT treated tRNA samples were separated on a 12.5% polyacrylamide TBE gel containing 50% urea. Samples were electro-transferred from gels onto a Biodyne B Nylon Membrane (Thermo Fisher) in 0.5x TBE buffer at 4 ˚C and crosslinked to the membrane by exposure to UV_{302} light for 3 minutes. Membranes were then pre-hybridized at 42˚C in ULTRAhyb-Oligo buffer (Thermo Fisher) for 1 hr and subsequently probed overnight with 2 pM of the respective biotin-labeled tRNA probe in ULTRAhyb-Oligo buffer. Membranes were washed twice with NorthernMax Low-stringency wash solution (Thermo Fisher) for 5 minutes at 42˚C followed by 2 subsequent 15-minute washes at 50˚C in NorthernMax High stringency wash solution (Thermo Fisher). Washed membranes were then blocked for 30 minutes at room temperature with Odyssey Blocking Buffer (LI-COR Biosciences) supplemented with 1% SDS. Biotin probes were detected by incubation with IRDye-800RD Streptavidin (LI-COR Biosciences) in Odyssey Blocking Buffer supplemented with 1% SDS for 30 minutes at room temperature. Membranes were washed 3 times in 1X PBS supplemented with 0.1% Tween-20 for 5 minutes and visualized with the Odyssey FC imaging system (LI-COR Biosciences). Images were captured and processed with the Image Studio™ software package (LI-COR Biosciences)

Murine infection models. For all animal infections, *P. aeruginosa* isolates were subcultured from overnight growth at a 1:50 dilution for 3 hr in MINS. Cells were pelleted, suspended in PBS and adjusted to an appropriate dose. For the mouse bacteremia model, 6 to 8-week-old BALBc female mice (Envigo) were anesthetized with 75 mg/kg ketamine and 5 mg/kg xylazine, and infected intranasally with 50 µl of the bacterial suspension. Mice were monitored every 8 hours for disease progression and euthanized prior to death by carbon dioxide inhalation. Survival curves were constructed by the Kaplan-Meier method (27) and compared using the Mantel-Cox (Log-rank) test (28). For the subcutaneous abscess model, 6 to 8-week-old C57BL/6J female mice (The Jackson Laboratory) were anesthetized as above. The area along the right rear flank was clipped, treated with a depilatory cream and cleansed with an antiseptic wipe. Mice were infected with 50 µl of the bacterial suspension by subcutaneous injection. The formation and size of an abscess was monitored daily. The abscess size was plotted as a function of time. Mean area-under-the-curve (AUC) values were calculated in Prism (GraphPad Software) and compared using an unpaired t-test (two-tailed).

The PABL isolates were grouped based upon their virulence in the mouse bacteremia infection model as described above. To determine the virulence grouping, BALB/c mice were infected by tail-vein injection as above at multiple doses (n = 5, minimum of 2 doses). Mice with pre-lethal illness, as determined by pre-defined criteria(29) were euthanized and scored as dead. The lowest infectious dose that resulted in < 50% survival was identified for each isolate. Isolates were then binned into groups based upon the aforementioned lethal dose. Virulence group 7 represented a pre-lethal dose between Log_{10} CFU 6.0 and 6.5, group 6 represented a pre-lethal dose between Log_{10} CFU 6.5 and 7.0, group 5 represented a pre-lethal dose between Log_{10} CFU 7.0 and 7.5, group 4 represented a pre-lethal dose between Log_{10} CFU 7.5 and 8.0, group 3 represented a pre-lethal dose between Log_{10} CFU 8.0 and 8.5, group 2 represented a pre-lethal dose between Log_{10} CFU 8.5 and 9.0, and group 1 represented a pre-lethal dose greater than Log_{10} CFU 9.0.

Mammalian cell infections. For cytotoxicity experiments, HeLa (ATCC) cells were seeded into 12-well polystyrene tissue culture plates (Corning) in DMEM supplemented with 10% fetal bovine serum (FBS). *P. aeruginosa* strains cultured overnight in LB were adjusted to a multiplicity of infection (MOI) of 10 in RPMI medium 1640 (Gibco). Confluent HeLa cells were washed in PBS, overlaid with 2 ml of the *P. aeruginosa* preparation and centrifuged at 750 x g to synchronize the infections. Infected cells were incubated at 37 ˚C in 5% CO_2. Fifty microliters of the media were removed at specified times and processed using a CytoTox 96® Non-radioactive cytotoxicity assay (Promega) per manufacturer instructions. Control cells were treated with 1% Triton X-100 to reach 100% cell lysis. The percentage of cytotoxicity was calculated relative to the lysis control as follows: 100 x (A_{490} sample – A_{490} uninfected cells) / (A_{490} Triton X-100 – A_{490} uninfected cells). For visualization, cells were fixed in 4% paraformaldehyde (1x PBS) for 15 min, washed with 1x PBS then stained with 1% crystal violet for 5 min. Stained cells were washed 5x with 1x PBS and visualized at 20x magnification using a Leica DMIRB inverted microscope fitted with a Leica DFC450C camera. Images were obtained using the Leica Application Suite v4.12.0 software package from a total of 10 fields of view (FOV) compiled from two independent experiments for each condition. Cells were identified with the "Analyze Particles" tool from ImageJ and analyzed for their circularity (degree of rounding) as part of the "Measurement" command(30). Circularity = 4pi(area/perimeter^2), ranging from 1.0 (a perfect circle) to 0.0 (an increasingly elongated polygon). Cells were considered to have substantial rounding with a circularity greater than 0.7. The percentage of cells with a circularity greater than 0.7 (cell rounding) was calculated for each FOV and analyzed for differences between groups using Prism (GraphPad).

For adhesion experiments, J774 murine macrophage-like (ATCC), HEK293T (human embryonic kidney) (ATCC) or HeLa cells (ATCC) were seeded into 24-well polystyrene tissue culture plates (Fisher Scientific) in DMEM supplemented with 10% FBS. *P. aeruginosa* strains were prepared as described above to reach a MOI of 10 and overlaid onto PBS washed cells. Infected cells were incubated for 3 hr after which they were washed 5 times with PBS and lysed in 0.1% Triton X-100. Serial dilutions of the lysates were plated for bacterial enumeration. The percentage adherence was calculated relative to the inoculum.

Mammalian Cell Transfections. Transfection experiments were performed using a modified procedure from Veesenmeyer et al.(31). HeLa cells were seeded into 24-well polystyrene tissue culture plates (Fisher Scientific) in DMEM supplemented with 10% FBS. Cells were grown overnight to 80% confluence. The culture media was refreshed with DMEM + 10% FBS 1 hour prior to transfection. Cells were transiently transfected with 1.5 µl of Lipofectamine 3000 (Invitrogen),1 µl of P3000 (Invitrogen) and 3 µg of plasmid DNA in 50 µl of Opti-MEM (Gibco). After 5 hours cells were refreshed with DMEM + 10% FBS and incubated for the indicated times. At the indicated times, supernatants were collected for detection of excreted lactate dehydrogenase, cells were washed twice with PBS and fixed for 10 min in 3.7% formaldehyde solution. Fixed cells were again washed and extracted with 0.1% Triton X-100 in PBS for 5 minutes. Cells were then stained for actin using 2.5% Texas Red^{TM}-X phalloidin (Thermo Fisher) for 20 minutes and 14 µM 4',6-diamidino-2-phenylindole (DAPI) for 5 min with PBS washes between each step. Cells were visualized using an EVOS® FL imaging system (Electron Microscopy Sciences) fitted with GFP, Tx-Red and DAPI filter cubes. The pEF1α-IRES-AcGFP1A transfection vector expresses GFP off of a bicistronic transcript from an internal ribosomal entry site (IRES), allowing for easy identification of transfected cells. Transfected cell (GFP) and actin stained (Texas Red) images were merged using ImageJ(30). Using the measure function of ImageJ, the ratio of the longest dimension (L) over the shortest dimension (S) for each transfected cell was calculated from the merged image. Data were obtained from a total of 8 fields of view (FOV) compiled from two independent experiments. Between 111 and 144 transfected cells for each condition were analyzed for cell shape. The L:S ratio was used as a surrogate for cell shape. Cells were considered to have substantial rounding with a L:S ratio less than 2. The percentage of cells with a L:S ratio less than 2 (cell rounding) was calculated for each FOV and analyzed for differences between groups using Prism (GraphPad).

In vitro nuclease assays. To assay for general DNA or RNA endonuclease activity, purified Cdi1A-CT^{PABL017} was diluted into either DNAase or RNAse Alert Buffer (IDT) at a 20 µM final concentration and incubated at 37˚C for 1 hr. The mixture was transferred to a 96-well black-walled assay plate

(Corning) and fluorescent spectra were measured on a SpectraMax® M3 microplate reader (Molecular Devices) per manufacturer instructions. DNAseI or RNAseI were used as positive controls. Substrates within the kits are synthetic oligonucleotides capped with a fluorescein molecule on one end and a dark quencher on the other end.

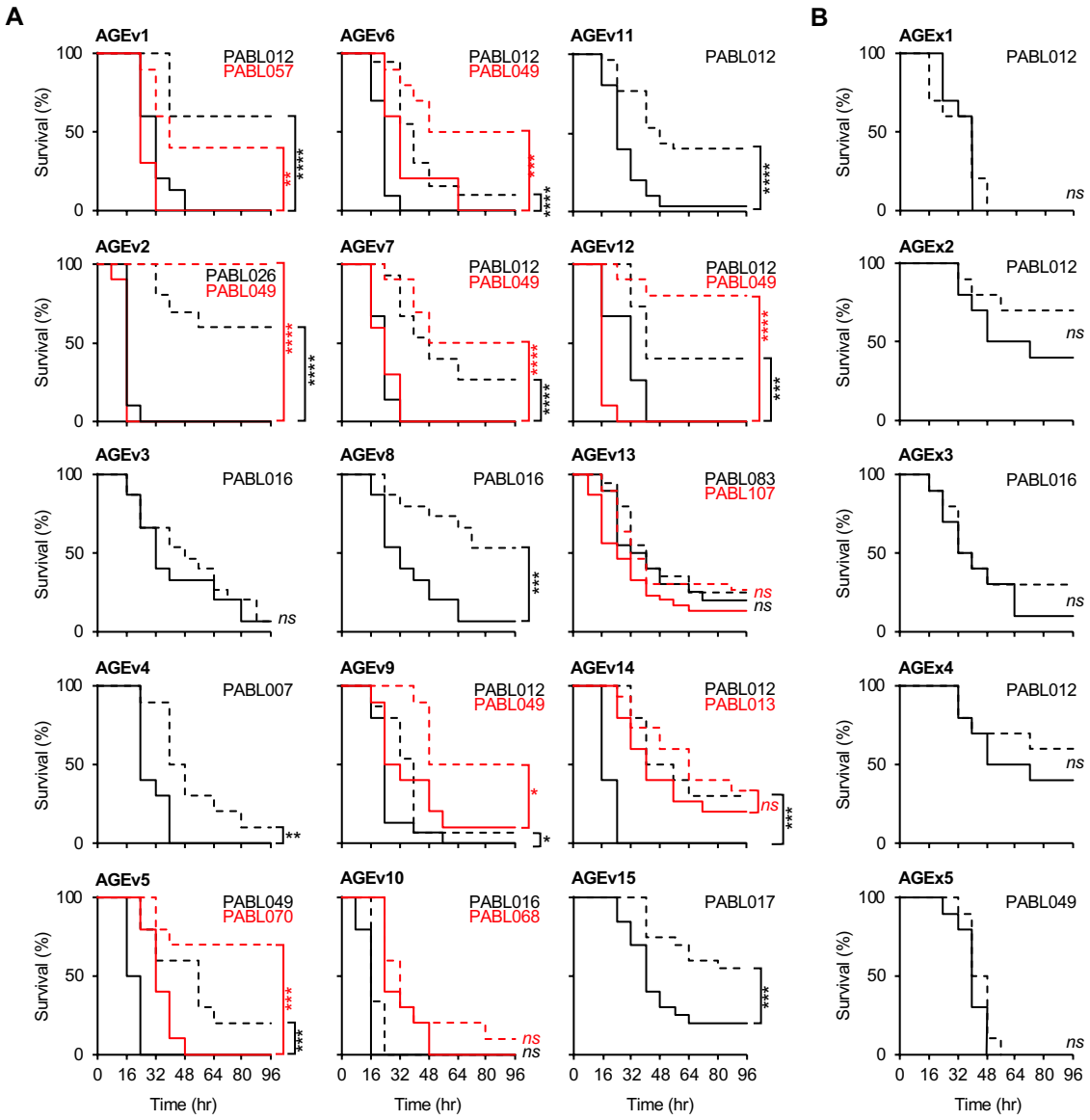

Fig. S1. Survival of mice infected with AGEv mutants. Mice were intravenously infected with a parental PABL isolate (solid lines) or an (A) AGEv or (B) AGEx mutant (dashed lines) and monitored for disease progression. When mutants were tested in a second *P. aeruginosa* strain background, these results are colored in red, respectively. Data were plotted on a Kaplan-Meier curve. Differences were analyzed for significance by the Mantel-Cox (LogRank) test. **P* < 0.05, ***P* < 0.01, ****P* < 0.001, *****P* < 0.0001 or *ns* (not significant) with n ≥ 10 mice per group.

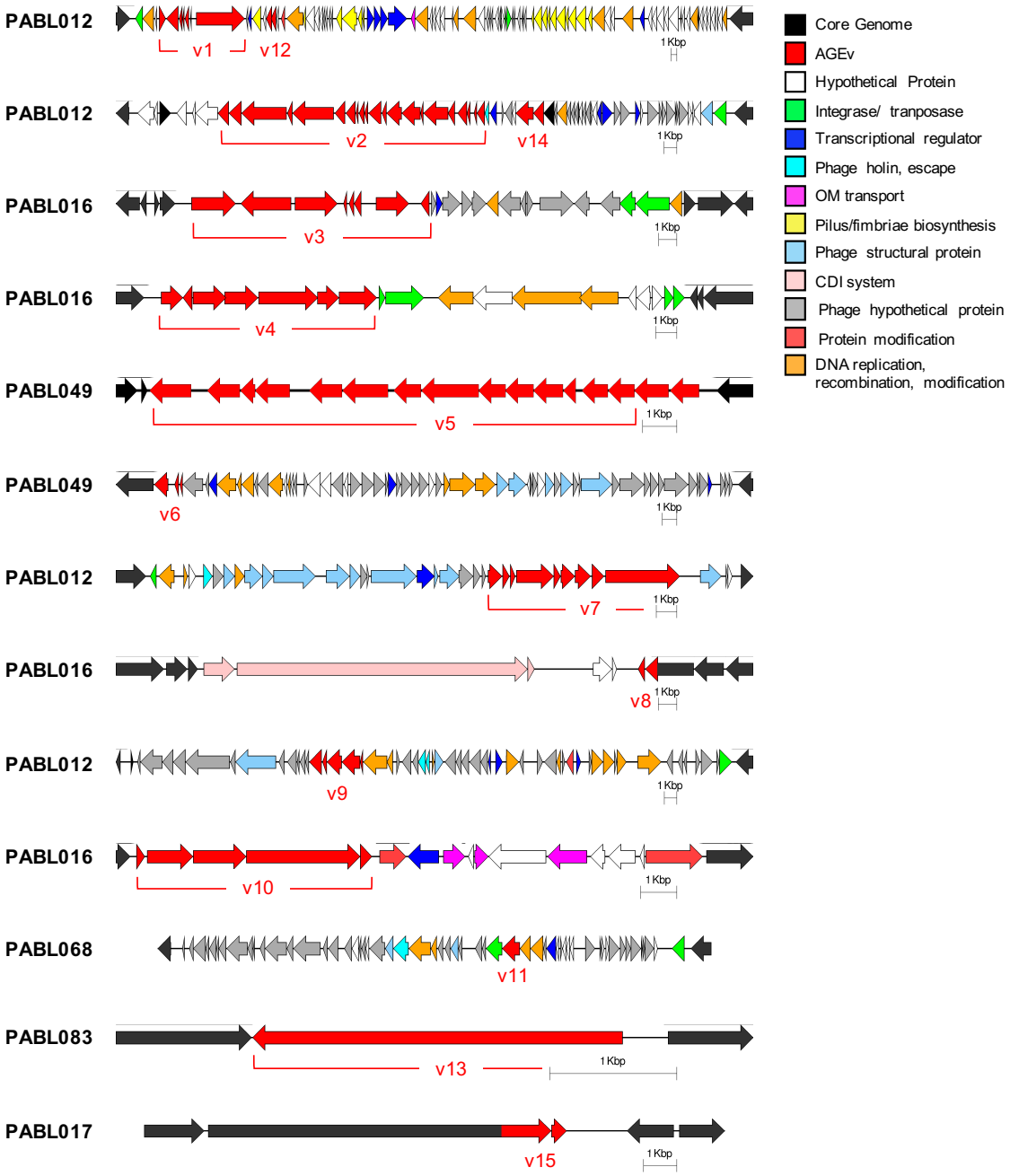

Fig. S2. The genomic context of AGEvs. The location of AGEvs within the genome of a representative isolate was determined by BLAST. AGEv names and predicted ORFs within the AGEv are colored in red (e.g. AGEv1 is labeled as “v1). Predicted open reading frames flanking the AGEv that are part of the accessory genome are colored according to annotated functions. The

genetic borders of the core genome surrounding the AGEv are colored in black. ORF annotations were edited in Artemis(4) and visualized using EasyFig (6).

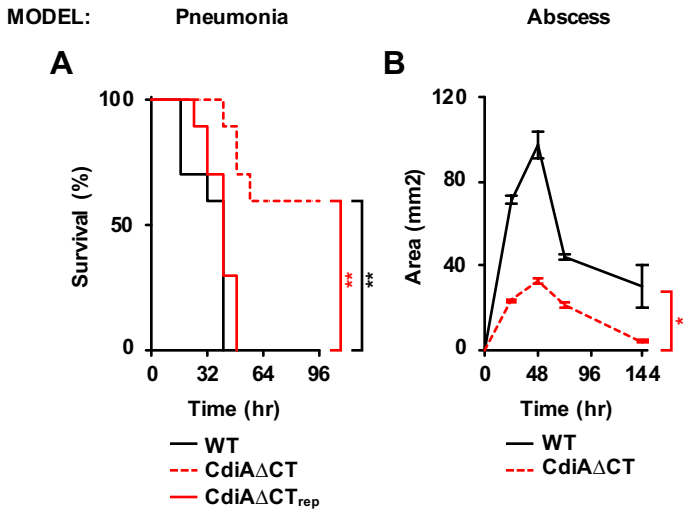

Fig. S3. ***P. aeruginosa*** **Cdi1A^{PABL017} functions in multiple infection models.** Mice were infected by (A) intranasal inoculation, or (B) subcutaneous injection with *P. aeruginosa* isolates PABL017 WT or the indicated *cdi1A* mutant strain. (A) Infected mice were monitored for disease progression over 96 hr. Data were plotted on a Kaplan-Meier curve. Differences were analyzed for significance by the Mantel-Cox (LogRank) test. $^{**}P < 0.01$, n ≥ 10 mice per group, rep (repaired mutation back to WT). (B) The area of the subcutaneous abscess (mm^2) was recorded over 144 hr. An unpaired t-test was performed with area under the curve measurements. $^{*}P < 0.05$, n ≥ 10 mice per group.

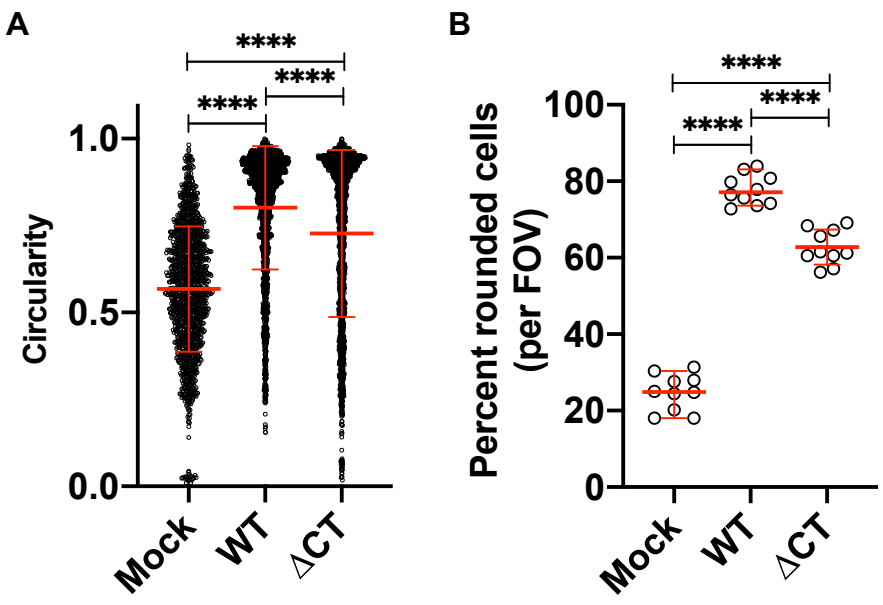
A
****
****
****
1.0
0.5
0.0
Circularity
Mock
WT
ΔCT
B
****
****
****
100
80
60
40
20
0
Percent rounded cells
(per FOV)
Mock
WT
ΔCT

C

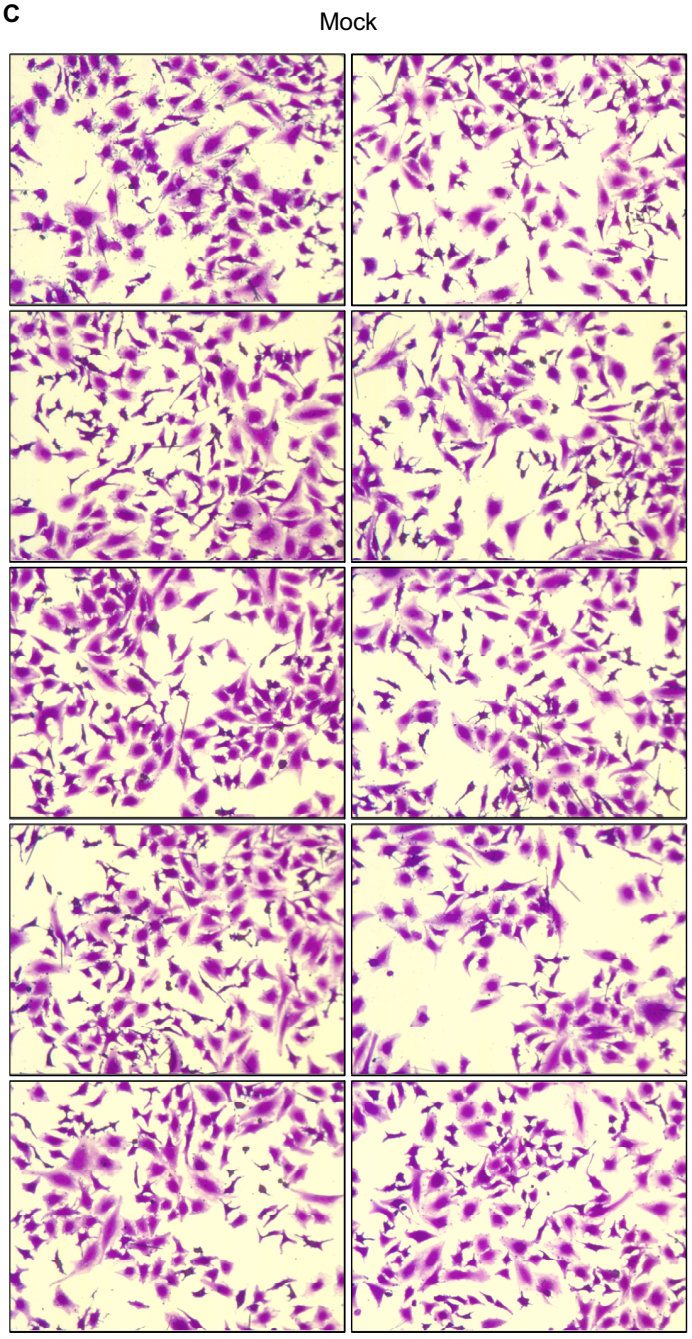

D

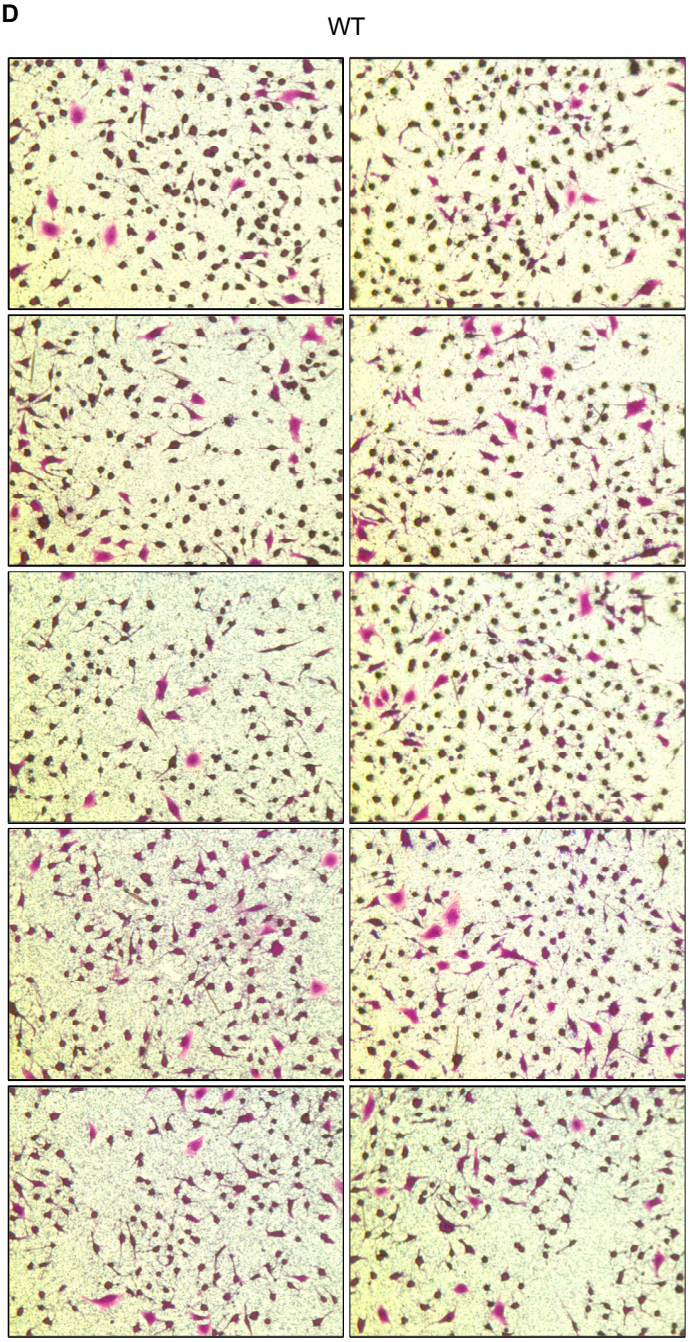

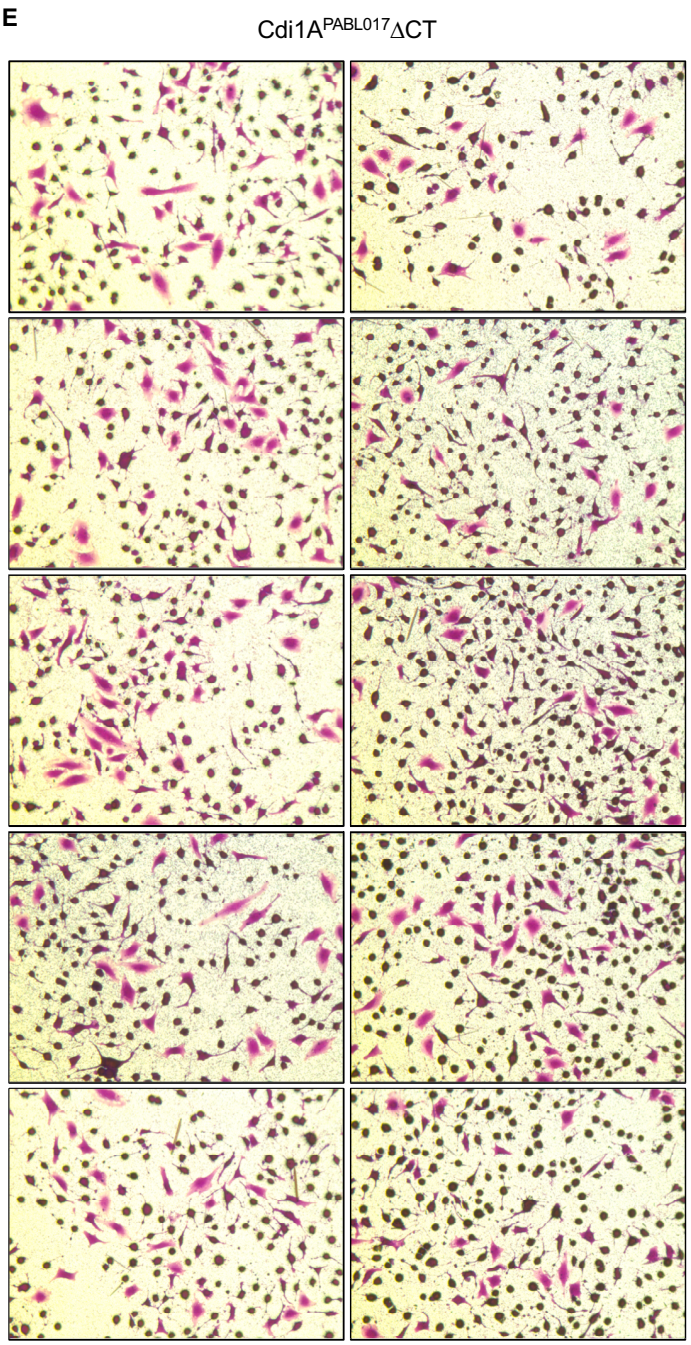

Fig.S4. *P. aeruginosa* Cdi1A^{PABL017} enhances to HeLa cell rounding. HeLa cells were infected with PABL017 WT or the Cdi1A^{PABL017}ΔCT mutant strain at a MOI of 10. Cells were fixed and stained

at 5 hours post-infection to visualize cell rounding. For each condition, over 1400 cells were analyzed from 10 fields of view (FOV) obtained from 2 independent experiments. (A) The degree of cell rounding (circularity) was determined for each cell using ImageJ (a value of 1 indicates a perfect circle). Individual data points are presented with means ± SD (Kruskal-Wallis test with Dunn's multiple comparisons, ****P < 0.0001). (B) The data were also analyzed for the percentage of round cells (circularity > 0.7) per FOV. Individual data points are presented as means ± SD (One-way ANOVA with Holm-Sidack's multiple comparisons, n = 10, ****P < 0.0001). The individual FOV images are tiled for Mock (C), WT (D) or Cdi1A$^{PABL017}\Delta$CT (E) infected cells.

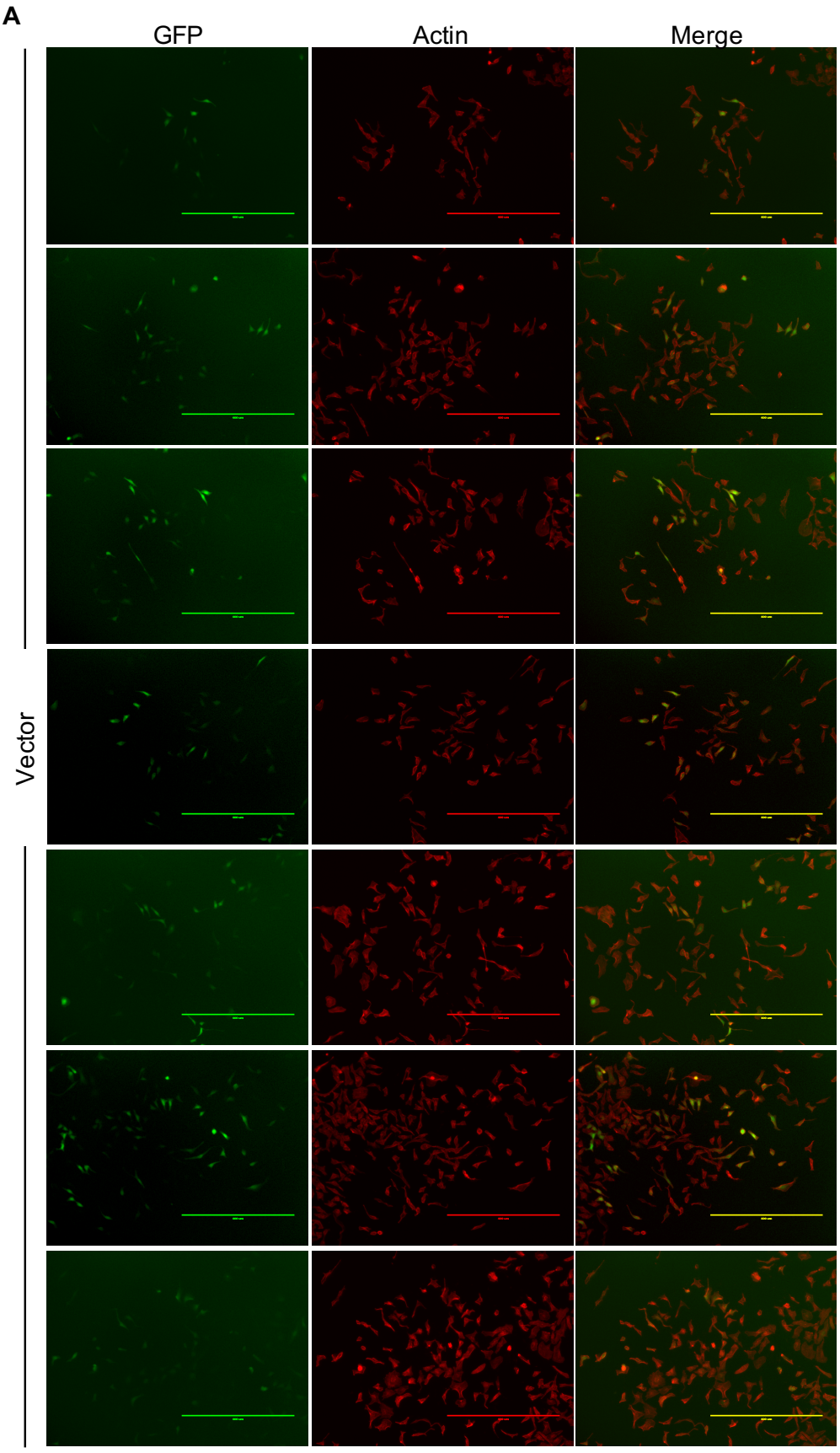
A
GFP
Actin
Merge
Vector

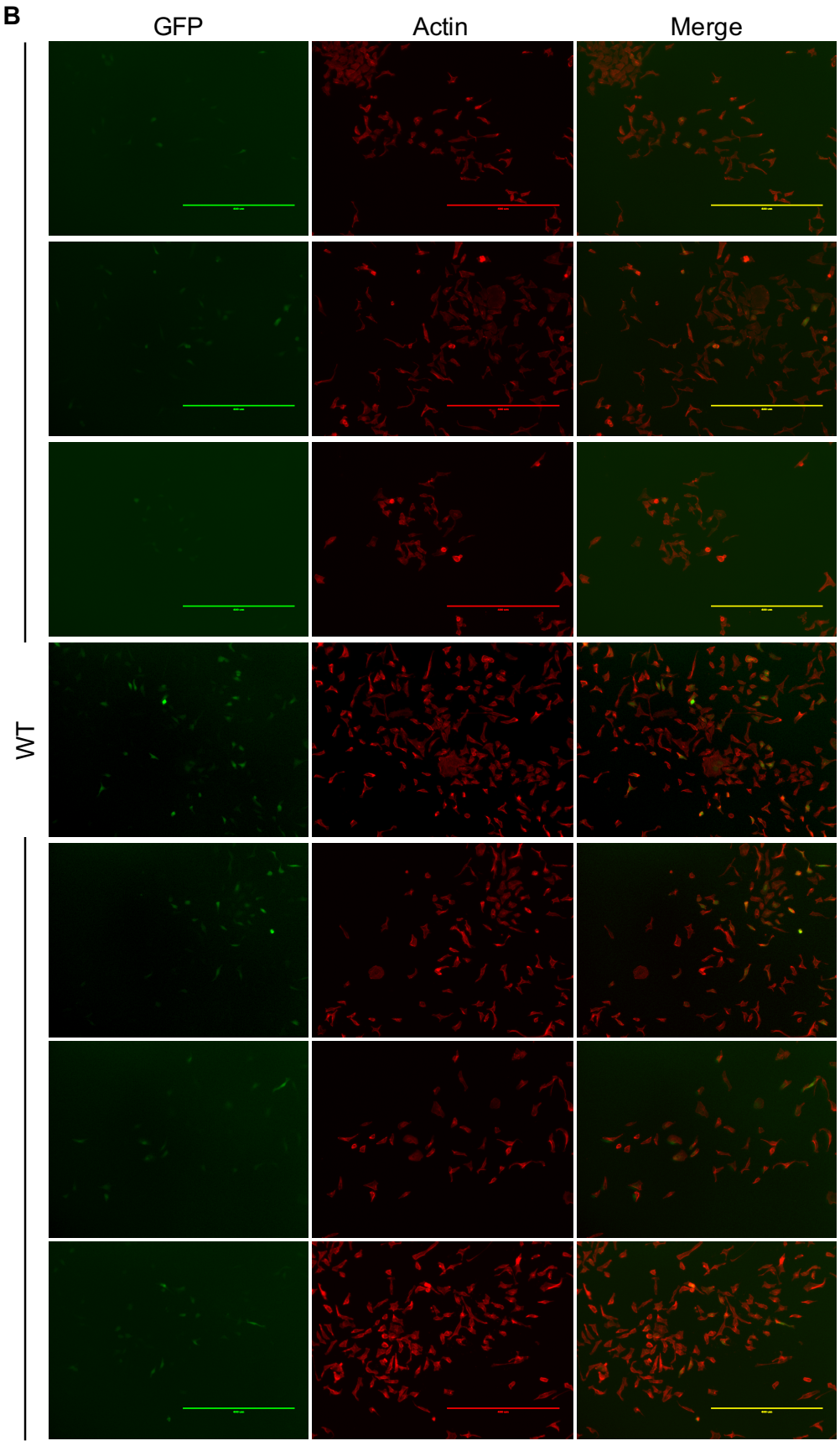
B
GFP
Actin
Merge
WT

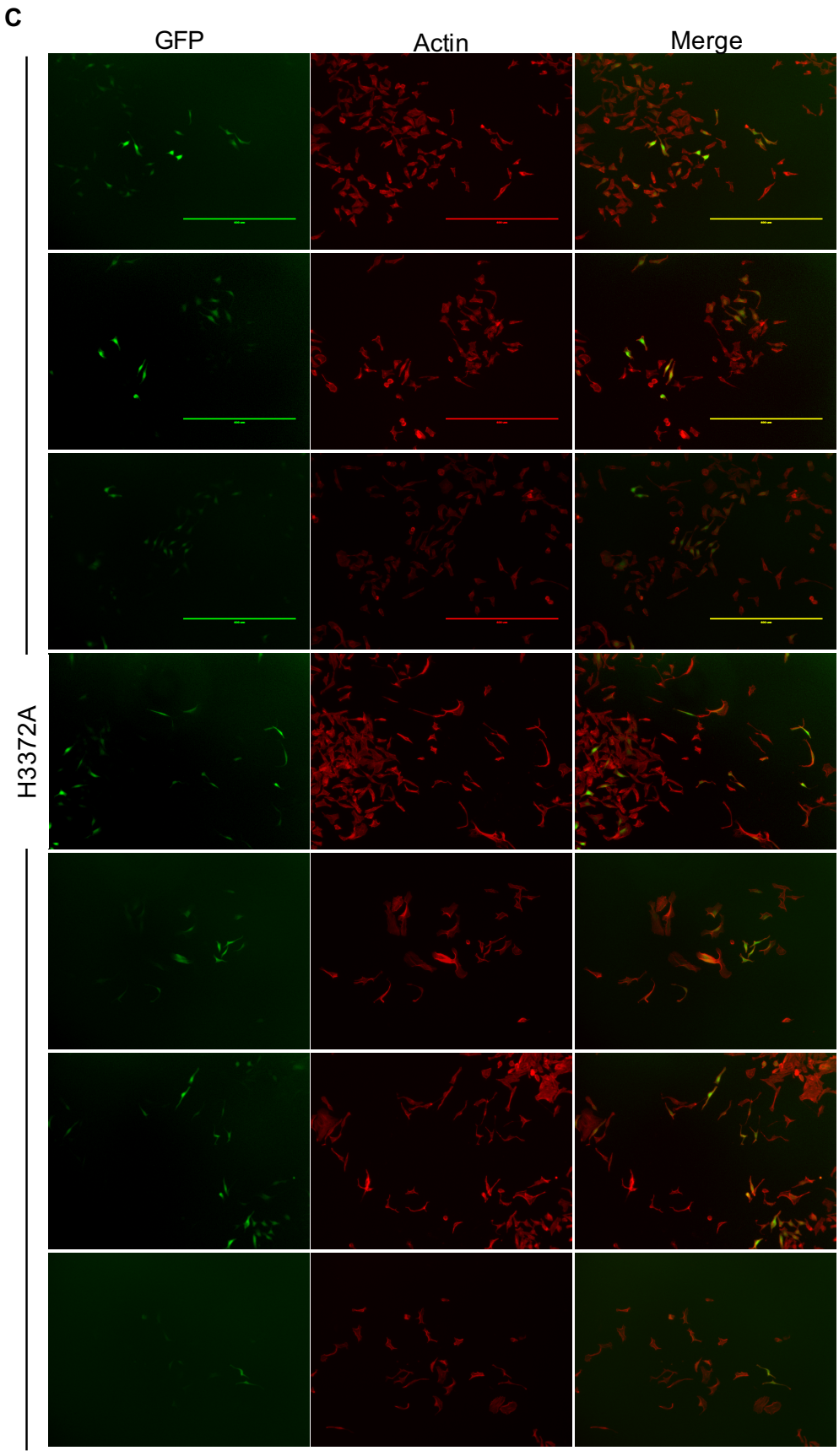
c
GFP
Actin
Merge
H3372A

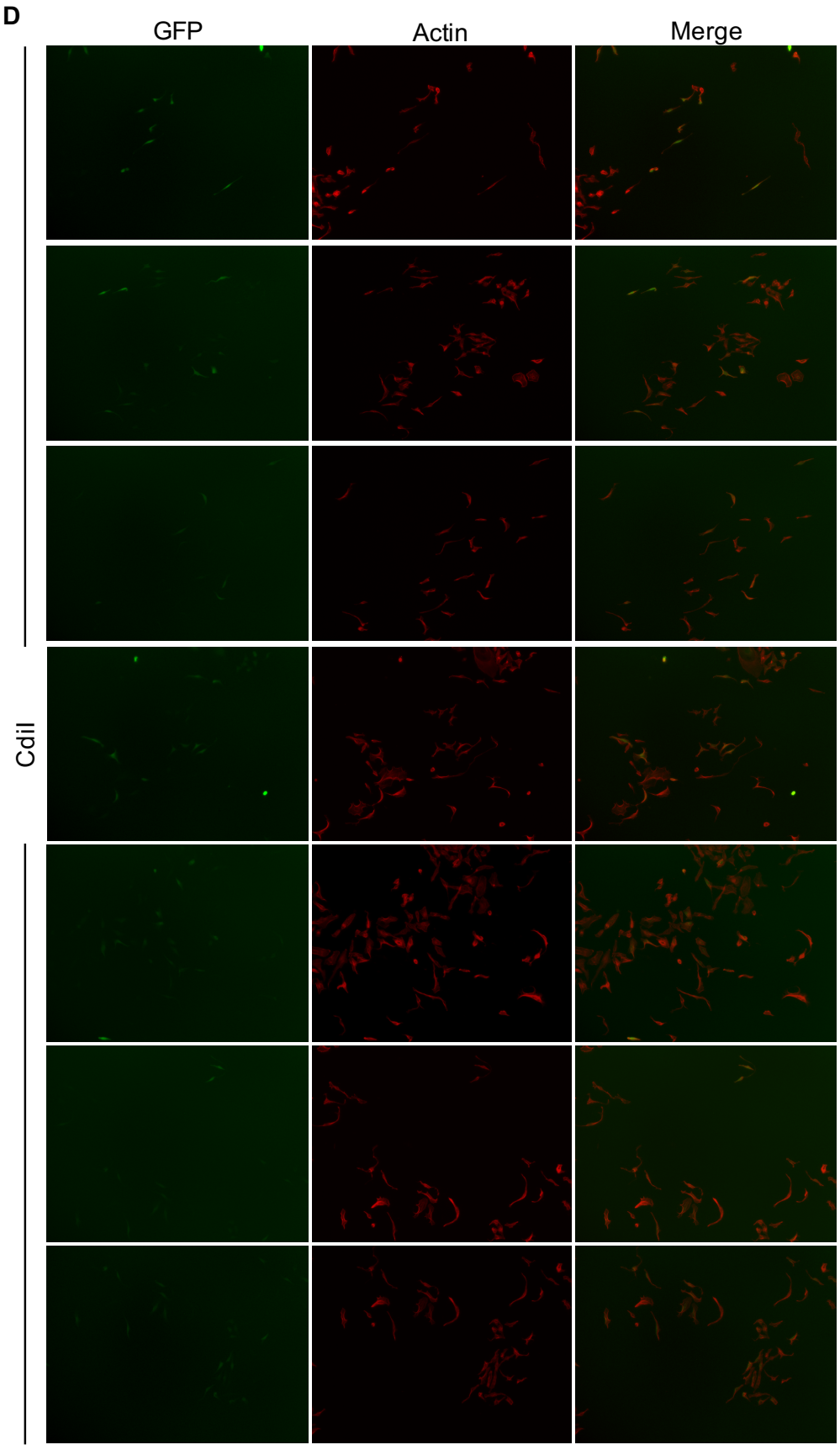
D
GFP
Actin
Merge
CdiI

Fig. S5. Additional images of transfected HeLa cells. HeLa cells were transfected with empty pEF1α-IRES-AcGFP1A (vector) (A), or vector containing the coding regions for Cdi1A-CT^{PABL017} (WT) (B), Cdi1A^{PABL017}-CT[H3372A] (H3372A) (C), or Cdi1I^{PABL017} (CdiI) (D). Cells were fixed, stained for actin, and visualized by fluorescence microscopy. Seven representative fields of view (FOV) are provided for each transfection condition.

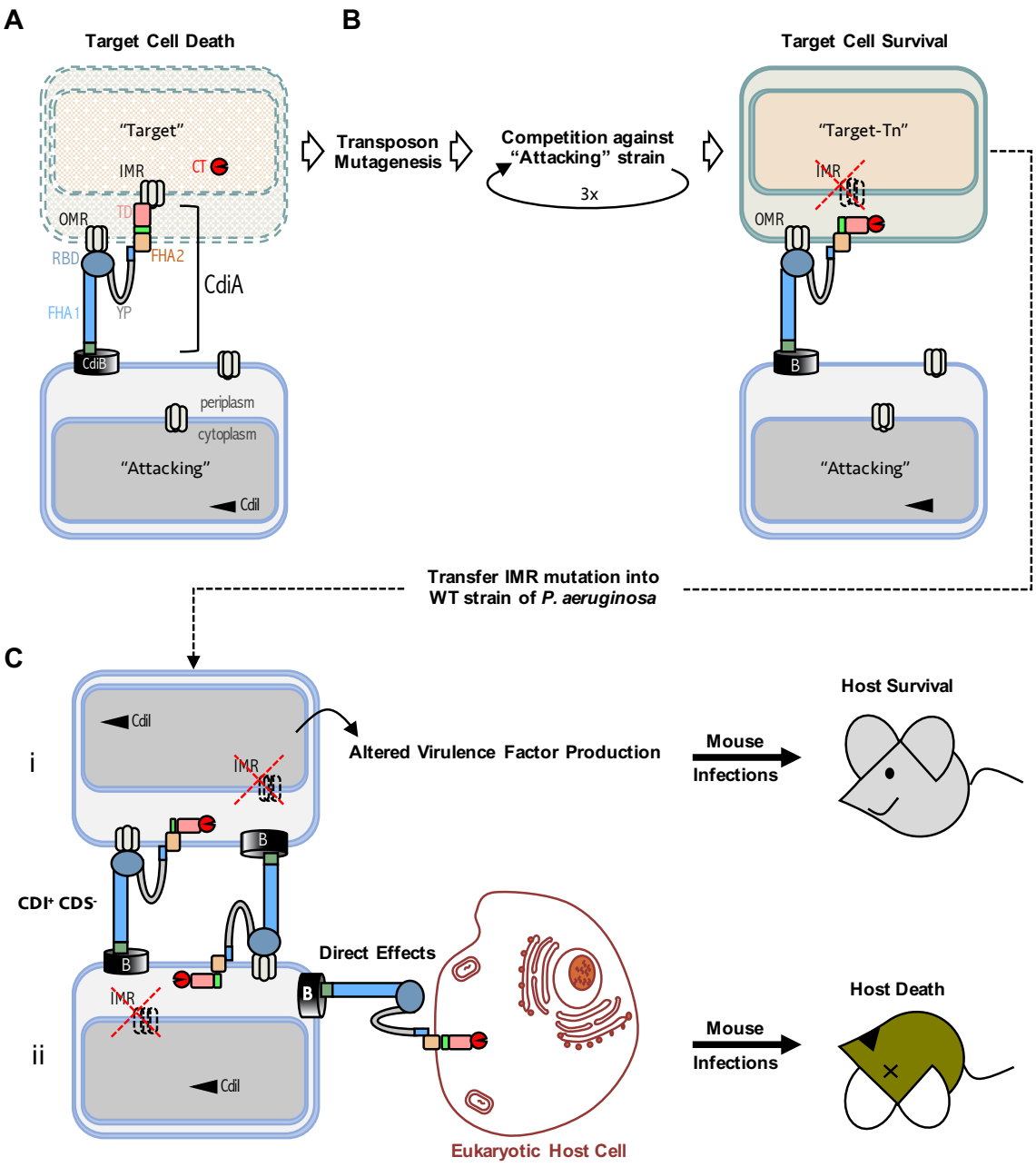

Fig. S6. Strategy to determine whether contact-dependent-signaling (CDS) is required for Cdi1A^{PABL017}-dependent virulence. (A) CdiA intoxication of a target cell occurs through a stepwise delivery mechanism. CdiA is first exported to the bacterial surface through a Type Vb secretion mechanism with the aid of an outer membrane β-barrel protein CdiB. Once properly positioned at the bacterial surface, CdiA-dependent targeting of a neighboring bacterium is initiated through interactions between a receptor binding domain (RBD), displayed at the distal end of the N-terminal

CdiA stalk (FHA1), and an outer membrane receptor (OMR) protein on the cell surface of the target bacterium(32, 33). Subsequent events mediated by the C-terminal CdiA translocation domains FHA2 and TD facilitate delivery of the CT across the outer and inner membranes respectively. It has been proposed that the FHA2 domain mediates translocation across the outer membrane(32) with translocation across the inner membrane requiring an interaction with an inner membrane receptor (IMR) in the target cell cytoplasmic membrane(32, 34). Abbreviations for CdiA: stalk formed by a putative β-helix structure (FHA1), receptor binding domain (RBD), tyrosine- and proline-rich region (YP), putative outer membrane translocation domain (FHA2), putative inner membrane translocation domain (TD), C-terminal toxin domain (CT). Abbreviations for the target cell: inner membrane receptor (IMR), outer membrane receptor (OMR). (B) To identify target cell receptors involved in uptake of the Cdi1A^{PABL017}-CT from an attacking cell, a transposon insertion library of the CDI susceptible target strain Cdi1AΔCT/I^{PABL017} was generated and subjected to 3 rounds of subsequent CDI with a parental PABL017 attacking strain. Transposon insertion sites within CDI-resistant mutants were identified by Illumina sequencing. It was anticipated that some transposon insertions would occur in genes that produce receptors involved in uptake of the Cdi1A^{PABL017}-CT, such as the IMR. (C) In-frame deletion mutations were generated in the PABL017 strain background to create a strain that capable of producing a functional Cdi1A^{PABL017} exoprotein (CDI^{+}) but resistant to uptake of a Cdi1A^{PABL017}-CT domain delivered by attacking cells (CDS^{-}). This mutant strain was tested for virulence in a mouse infection model to determine (i) whether uptake of a Cdi1A^{PABL017}-CT domain (i.e. CDS) was required for virulence or (ii) whether Cdi1A^{PABL017} may have a direct effect on host cells.

Table S1. Bacterial strain list.

Species	Strain	Relevant Characteristics	Reference
E. coli	Top10	F- *mcrA* Δ(*mrr-hsdRMS-mcrBC*) φ80*lacZ*ΔM15 Δ*lacX74 nupG recA1 araD139* Δ(*ara-leu*)7697 *galE15 galK16 rpsL*(StrR) *endA1* λ-	Invitrogen
E. coli	S17.1 λpir	TpR SmR *recA*, *thi*, *pro*, *hsdR*-M+RP4: 2-Tc:Mu: Km Tn7 λpir	Simon (1983)[a]
E. coli	BL21(DE3)	F– *ompT gal dcm lon hsdSB*(rB–mB–) λ(DE3 [*lacI lacUV5*-T7p07 *ind1 sam7 nin5*]) [*malB*+]K-12(λS)	Invitrogen
P. aeruginosa	PABL001	human bacteremia isolate; Assembly: GCA_003412325.1	Scheetz (2009)[b]
P. aeruginosa	PABL002	human bacteremia isolate; Assembly: GCA_003412285.1	Scheetz (2009)
P. aeruginosa	PABL003	human bacteremia isolate; Assembly: GCA_003412295.1	Scheetz (2009)
P. aeruginosa	PABL004	human bacteremia isolate; Assembly: GCA_003411985.1	Scheetz (2009)
P. aeruginosa	PABL006	human bacteremia isolate; Assembly: GCA_003412035.1	Scheetz (2009)
P. aeruginosa	PABL007	human bacteremia isolate; Assembly: GCA_003411765.1	Scheetz (2009)
P. aeruginosa	PABL009	human bacteremia isolate; Assembly: GCA_003411645.1	Scheetz (2009)
P. aeruginosa	PABL010	human bacteremia isolate; Assembly: GCA_003411955.1	Scheetz (2009)
P. aeruginosa	PABL011	human bacteremia isolate; Assembly: GCA_003412275.1	Scheetz (2009)
P. aeruginosa	PABL012	human bacteremia isolate; Assembly: GCA_003429185.1	Scheetz (2009)
P. aeruginosa	PABL013	human bacteremia isolate; Assembly: GCA_003412255.1	Scheetz (2009)
P. aeruginosa	PABL014	human bacteremia isolate; Assembly: GCA_003412225.1	Scheetz (2009)
P. aeruginosa	PABL015	human bacteremia isolate; Assembly: GCA_003412215.1	Scheetz (2009)
P. aeruginosa	PABL016	human bacteremia isolate; Assembly: GCA_003412165.1	Scheetz (2009)
P. aeruginosa	PABL017	human bacteremia isolate; Assembly: GCA_003429205.1	Scheetz (2009)
P. aeruginosa	PABL018	human bacteremia isolate; Assembly: GCA_003412045.1	Scheetz (2009)
P. aeruginosa	PABL019	human bacteremia isolate; Assembly: GCA_003412155.1	Scheetz (2009)
P. aeruginosa	PABL020	human bacteremia isolate; Assembly: GCA_003412145.1	Scheetz (2009)
P. aeruginosa	PABL021	human bacteremia isolate; Assembly: GCA_003412075.1	Scheetz (2009)
P. aeruginosa	PABL022	human bacteremia isolate; Assembly: GCA_003412125.1	Scheetz (2009)
P. aeruginosa	PABL023	human bacteremia isolate; Assembly: GCA_003411725.1	Scheetz (2009)
P. aeruginosa	PABL024	human bacteremia isolate; Assembly: GCA_003411815.1	Scheetz (2009)
P. aeruginosa	PABL026	human bacteremia isolate; Assembly: GCA_003411355.1	Scheetz (2009)
P. aeruginosa	PABL027	human bacteremia isolate; Assembly: GCA_003411365.1	Scheetz (2009)
P. aeruginosa	PABL028	human bacteremia isolate; Assembly: GCA_003411845.1	Scheetz (2009)
P. aeruginosa	PABL029	human bacteremia isolate; Assembly: GCA_003412085.1	Scheetz (2009)
P. aeruginosa	PABL030	human bacteremia isolate; Assembly: GCA_003412115.1	Scheetz (2009)
P. aeruginosa	PABL031	human bacteremia isolate; Assembly: GCA_003411975.1	Scheetz (2009)
P. aeruginosa	PABL032	human bacteremia isolate; Assembly: GCA_003411965.1	Scheetz (2009)
P. aeruginosa	PABL033	human bacteremia isolate; Assembly: GCA_003411905.1	Scheetz (2009)
P. aeruginosa	PABL034	human bacteremia isolate; Assembly: GCA_003411895.1	Scheetz (2009)
P. aeruginosa	PABL035	human bacteremia isolate; Assembly: GCA_003411885.1	Scheetz (2009)
P. aeruginosa	PABL036	human bacteremia isolate; Assembly: GCA_003411875.1	Scheetz (2009)
P. aeruginosa	PABL037	human bacteremia isolate; Assembly: GCA_003411125.1	Scheetz (2009)
P. aeruginosa	PABL038	human bacteremia isolate; Assembly: GCA_003411665.1	Scheetz (2009)
P. aeruginosa	PABL040	human bacteremia isolate; Assembly: GCA_003411465.1	Scheetz (2009)
P. aeruginosa	PABL041	human bacteremia isolate; Assembly: GCA_003411235.1	Scheetz (2009)
P. aeruginosa	PABL042	human bacteremia isolate; Assembly: GCA_003411505.1	Scheetz (2009)
P. aeruginosa	PABL043	human bacteremia isolate; Assembly: GCA_003411445.1	Scheetz (2009)
P. aeruginosa	PABL044	human bacteremia isolate; Assembly: GCA_003411585.1	Scheetz (2009)
P. aeruginosa	PABL045	human bacteremia isolate; Assembly: GCA_003411535.1	Scheetz (2009)
P. aeruginosa	PABL046	human bacteremia isolate; Assembly: GCA_003411805.1	Scheetz (2009)
P. aeruginosa	PABL047	human bacteremia isolate; Assembly: GCA_003411785.2	Scheetz (2009)
P. aeruginosa	PABL048	human bacteremia isolate; Assembly: GCA_003411745.1	Scheetz (2009)
P. aeruginosa	PABL049	human bacteremia isolate; Assembly: GCA_003411695.1	Scheetz (2009)
P. aeruginosa	PABL051	human bacteremia isolate; Assembly: GCA_003411705.1	Scheetz (2009)
P. aeruginosa	PABL052	human bacteremia isolate; Assembly: GCA_003411635.1	Scheetz (2009)
P. aeruginosa	PABL053	human bacteremia isolate; Assembly: GCA_003411595.1	Scheetz (2009)
P. aeruginosa	PABL054	human bacteremia isolate; Assembly: GCA_003411555.1	Scheetz (2009)
P. aeruginosa	PABL055	human bacteremia isolate; Assembly: GCA_003411245.1	Scheetz (2009)
P. aeruginosa	PABL056	human bacteremia isolate; Assembly: GCA_003411195.1	Scheetz (2009)
P. aeruginosa	PABL057	human bacteremia isolate; Assembly: GCA_003410785.1	Scheetz (2009)
P. aeruginosa	PABL058	human bacteremia isolate; Assembly: GCA_003411095.1	Scheetz (2009)
P. aeruginosa	PABL059	human bacteremia isolate; Assembly: GCA_003410745.1	Scheetz (2009)
P. aeruginosa	PABL060	human bacteremia isolate; Assembly: GCA_003411345.1	Scheetz (2009)
P. aeruginosa	PABL061	human bacteremia isolate; Assembly: GCA_003410975.1	Scheetz (2009)
P. aeruginosa	PABL062	human bacteremia isolate; Assembly: GCA_003411565.1	Scheetz (2009)
P. aeruginosa	PABL063	human bacteremia isolate; Assembly: GCA_003411475.1	Scheetz (2009)
P. aeruginosa	PABL064	human bacteremia isolate; Assembly: GCA_003411425.1	Scheetz (2009)
P. aeruginosa	PABL065	human bacteremia isolate; Assembly: GCA_003411415.1	Scheetz (2009)

P. aeruginosa	PABL066	human bacteremia isolate; Assembly: GCA_003411335.1	Scheetz (2009)
P. aeruginosa	PABL067	human bacteremia isolate; Assembly: GCA_003411275.1	Scheetz (2009)
P. aeruginosa	PABL068	human bacteremia isolate; Assembly: GCA_003411285.1	Scheetz (2009)
P. aeruginosa	PABL069	human bacteremia isolate; Assembly: GCA_003411265.1	Scheetz (2009)
P. aeruginosa	PABL070	human bacteremia isolate; Assembly: GCA_003410625.1	Scheetz (2009)
P. aeruginosa	PABL071	human bacteremia isolate; Assembly: GCA_003410875.1	Scheetz (2009)
P. aeruginosa	PABL072	human bacteremia isolate; Assembly: GCA_003410715.1	Scheetz (2009)
P. aeruginosa	PABL073	human bacteremia isolate; Assembly: GCA_003411025.1	Scheetz (2009)
P. aeruginosa	PABL074	human bacteremia isolate; Assembly: GCA_003410855.1	Scheetz (2009)
P. aeruginosa	PABL075	human bacteremia isolate; Assembly: GCA_003410765.1	Scheetz (2009)
P. aeruginosa	PABL076	human bacteremia isolate; Assembly: GCA_003411165.1	Scheetz (2009)
P. aeruginosa	PABL077	human bacteremia isolate; Assembly: GCA_003411185.1	Scheetz (2009)
P. aeruginosa	PABL078	human bacteremia isolate; Assembly: GCA_003411145.1	Scheetz (2009)
P. aeruginosa	PABL079	human bacteremia isolate; Assembly: GCA_003411115.1	Scheetz (2009)
P. aeruginosa	PABL080	human bacteremia isolate; Assembly: GCA_003411045.1	Scheetz (2009)
P. aeruginosa	PABL081	human bacteremia isolate; Assembly: GCA_003411035.1	Scheetz (2009)
P. aeruginosa	PABL082	human bacteremia isolate; Assembly: GCA_003411005.1	Scheetz (2009)
P. aeruginosa	PABL083	human bacteremia isolate; Assembly: GCA_003410985.1	Scheetz (2009)
P. aeruginosa	PABL084	human bacteremia isolate; Assembly: GCA_003410935.1	Scheetz (2009)
P. aeruginosa	PABL085	human bacteremia isolate; Assembly: GCA_003410925.1	Scheetz (2009)
P. aeruginosa	PABL086	human bacteremia isolate; Assembly: GCA_003410905.1	Scheetz (2009)
P. aeruginosa	PABL088	human bacteremia isolate; Assembly: GCA_003410645.1	Scheetz (2009)
P. aeruginosa	PABL089	human bacteremia isolate; Assembly: GCA_003410505.1	Scheetz (2009)
P. aeruginosa	PABL090	human bacteremia isolate; Assembly: GCA_003412365.1	Scheetz (2009)
P. aeruginosa	PABL091	human bacteremia isolate; Assembly: GCA_003410435.1	Scheetz (2009)
P. aeruginosa	PABL092	human bacteremia isolate; Assembly: GCA_003410845.1	Scheetz (2009)
P. aeruginosa	PABL093	human bacteremia isolate; Assembly: GCA_003410835.1	Scheetz (2009)
P. aeruginosa	PABL094	human bacteremia isolate; Assembly: GCA_003410805.1	Scheetz (2009)
P. aeruginosa	PABL095	human bacteremia isolate; Assembly: GCA_003412355.1	Scheetz (2009)
P. aeruginosa	PABL096	human bacteremia isolate; Assembly: GCA_003410705.1	Scheetz (2009)
P. aeruginosa	PABL097	human bacteremia isolate; Assembly: GCA_003410695.1	Scheetz (2009)
P. aeruginosa	PABL098	human bacteremia isolate; Assembly: GCA_003410635.1	Scheetz (2009)
P. aeruginosa	PABL100	human bacteremia isolate; Assembly: GCA_003410595.1	Scheetz (2009)
P. aeruginosa	PABL101	human bacteremia isolate; Assembly: GCA_003410585.1	Scheetz (2009)
P. aeruginosa	PABL102	human bacteremia isolate; Assembly: GCA_003410515.1	Scheetz (2009)
P. aeruginosa	PABL103	human bacteremia isolate; Assembly: GCA_003410565.1	Scheetz (2009)
P. aeruginosa	PABL104	human bacteremia isolate; Assembly: GCA_003410445.1	Scheetz (2009)
P. aeruginosa	PABL105	human bacteremia isolate; Assembly: GCA_003410555.1	Scheetz (2009)
P. aeruginosa	PABL106	human bacteremia isolate; Assembly: GCA_003410475.1	Scheetz (2009)
P. aeruginosa	PABL107	human bacteremia isolate; Assembly: GCA_003410485.1	Scheetz (2009)
P. aeruginosa	PABL108	human bacteremia isolate; Assembly: GCA_003412325.1	Scheetz (2009)
P. aeruginosa	JPA001	PABL012 ΔAGEv1::Gm; made with pJA004	This Study
P. aeruginosa	JPA002	PABL057 ΔAGEv1::Gm; made with pJA004	This Study
P. aeruginosa	JPA004	PABL026 ΔAGEv2::Gm; made with pJA006	This Study
P. aeruginosa	JPA005	PABL049 ΔAGEv2::Gm; made with pJA007	This Study
P. aeruginosa	JPA006	PABL016 ΔAGEv3::Gm; made with pJA008	This Study
P. aeruginosa	JPA007	PABL007 ΔAGEv4::Gm; made with pJA009	This Study
P. aeruginosa	JPA009	PABL049 ΔAGEv5::Gm; made with pJA011	This Study
P. aeruginosa	JPA010	PABL070 ΔAGEv5::Gm; made with pJA011	This Study
P. aeruginosa	JPA011	PABL012 ΔAGEv6::Gm; made with pJA012	This Study
P. aeruginosa	JPA012	PABL049 ΔAGEv6::Gm; made with pJA013	This Study
P. aeruginosa	JPA013	PABL012 ΔAGEv7::Gm; made with pJA014	This Study
P. aeruginosa	JPA014	PABL049 ΔAGEv7::Gm; made with pJA015	This Study
P. aeruginosa	JPA015	PABL016 ΔAGEv8::Gm; made with pJA016	This Study
P. aeruginosa	JPA016	PABL012 ΔAGEv9::Gm; made with pJA017	This Study
P. aeruginosa	JPA017	PABL049 ΔAGEv9::Gm; made with pJA018	This Study
P. aeruginosa	JPA018	PABL016 ΔAGEv10::Gm; made with pJA019	This Study
P. aeruginosa	JPA019	PABL068 ΔAGEv10::Gm; made with pJA019	This Study
P. aeruginosa	JPA020	PABL012 ΔAGEv11:Gm; made with pJA020	This Study
P. aeruginosa	JPA021	PABL012 ΔAGEv12::Gm; made with pJA022	This Study
P. aeruginosa	JPA022	PABL049 ΔAGEv12::Gm; made with pJA023	This Study
P. aeruginosa	JPA023	PABL083 ΔAGEv13::Gm; made with pJA024	This Study
P. aeruginosa	JPA024	PABL107 ΔAGEv13::Gm; made with pJA025	This Study
P. aeruginosa	JPA025	PABL012 ΔAGEv14::Gm; made with pJA026	This Study
P. aeruginosa	JPA026	PABL013 ΔAGEv14::Gm; made with pJA026	This Study
P. aeruginosa	JPA027	PABL017 ΔAGEv15::Gm; made with pJA027	This Study
P. aeruginosa	JPA029	PABL012 ΔAGEx1::FLPscar; made with pJA028	This Study
P. aeruginosa	JPA030	PABL012 ΔAGEx2::FLPscar; made with pJA029	This Study
P. aeruginosa	JPA031	PABL016 ΔAGEx3::FLPscar; made with pJA030	This Study
P. aeruginosa	JPA032	PABL012 ΔAGEx4::FLPscar; made with pJA031	This Study

P. aeruginosa	JPA033	PABL049 ΔAGEx5::FLPscar; made with pJA032	This Study
P. aeruginosa	JPA035	PABL017 CdiAΔCT::Gm; made with pJA034	This Study
P. aeruginosa	JPA036	JPA035 with Gm removed by pFLP2 (FRT scar)	This Study
P. aeruginosa	JPA038	PABL017 attCTX::lacZ; made with miniCTX1-LacZ	This Study
P. aeruginosa	JPA039	PABL017 attCTX::Gm; made with miniCTX1-Gm	This Study
P. aeruginosa	JPA040	PABL017 CdiAΔCT; made with pJA050	This Study
P. aeruginosa	JPA041	PABL017 CdiAΔCTΔcdiI; made with pJA051	This Study
P. aeruginosa	JPA042	PABL017 CdiA [H3372A]; made with pJA052	This Study
P. aeruginosa	JPA043	JPA036 + *attCTX*::pBAD_*cdiI*^{PABL017}; made with pJA003	This Study
P. aeruginosa	JPA044	JPA040 repaired to PABL017 WT; made with pJA053	This Study
P. aeruginosa	JPA045	JPA041 repaired to PABL017 WT; made with pJA054	This Study
P. aeruginosa	JPA046	JPA042 repaired to PABL017 WT; made with pJA053	This Study
P. aeruginosa	JPA047	PABL017 Δ*dppBC*; made with pJA059	This Study
P. aeruginosa	JPA048	JPA040 Δ*dppBC*; made with pJA059	This Studv
P. aeruginosa	JPA049	JPA041 Δ*dppBC*; made with pJA059	This Study
P. aeruginosa	JPA050	JPA047 attCTX::Gm; made with miniCTX1-Gm	This Study
P. aeruginosa	JPA051	JPA048 attCTX::Gm; made with miniCTX1-Gm	This Study
P. aeruginosa	JPA052	JPA049 attCTX::Gm; made with miniCTX1-Gm	This Study
P. aeruginosa	JPA054	JPA040 + attCTX::Gm; made with miniCTX1-Gm	This Study
P. aeruginosa	JPA055	JPA044 + attCTX::Gm; made with miniCTX1-Gm	This Study
P. aeruginosa	JPA056	JPA041 + attCTX::Gm; made with miniCTX1-Gm	This Study
P. aeruginosa	JPA057	JPA045 + attCTX::Gm; made with miniCTX1-Gm	This Study

Table S2. Plasmids used in this study.

Plasmid	Relevant Characteristics (Description; oligos used; DNA template)	Reference
pMCSG53-ccdB	Apr, 6xHis-TEV, T7pro	Eschenfeldt, 2013
pEX18.AP	Apr, *oriT*, *sacB*, *lacZα*, MCS from pUC18	Hoang 1998
pEX18.GM	Gmr, *oriT*, *sacB*, *lacZα*, MCS from pUC18	Hoang 1998
pFLP2	Apr, *oriT*, *sacB*, Flp recombinase	Hoang 1998
miniCTX1	Tcr, integration vector, *Ω-FRT-attP*-MCS, *ori*, *int*, and *oriT*	Hoang 2000
miniCTX1-LacZ	*lacZ* at MCS of miniCTX1	Hoang 2000
miniCTX1-GmR	pUC-GM SmaI fragment (Gmr) into miniCTX1 SmaI	Gift (J. Mekalanos)
pEF1α-IRES-AcGFP1A	$P_{EF1\alpha}$-MCS-IRES2-AcGFP1, SV40 polyA, ori_{SV40}, ori_{SV40}, Kanr/Neor	Clontech
pTKRED	*araBAD* promoter	Addgene
pBT20	Mini transposon vector with Himar-1 mariner transposase	Kulasekara 2004
pJPA1	pFLP2 KpnI/HindIII (Apr, *oriT*, *sacB*), pBAD; oligos167,168; pTKRED	This Study
pJA001	miniCTX1 (Φ-FRT, *ori*, *int*, and *oriT*)+GmR; oligos161,162,163,164; PABL017 GenDNA	This Study
pJA002	pJPA1 expressing CdiIPABL017; oligos169, 170; PABL017 GenDNA	This Study
pJA003	miniCTX_pBAD_CdiIPABL017; oligos171, 172; PABL017 GenDNA	This Study
pJA004	pEX18.Ap PABL012 ΔAGEv1::Gmr; oligos1, 2, 3, 4,163, 164; PABL012 GenDNA, pJA001	This Study
pJA006	pEX18.Ap PABL026 ΔAGEv2::Gmr; oligos5, 6, 7, 8,163, 164; PABL026 GenDNA, pJA001	This Study
pJA007	pEX18.Ap PABL049 ΔAGEv2::Gmr; oligos13, 14, 15, 16,163, 164; PABL049 GenDNA, pJA001	This Study
pJA008	pEX18.Ap PABL016 ΔAGEv3::Gmr; oligos17, 18, 19, 20,163, 164; PABL016 GenDNA, pJA001	This Study
pJA009	pEX18.Ap PABL007 ΔAGEv4::Gmr; oligos25, 26, 27, 28,163, 164; PABL007 GenDNA, pJA001	This Study
pJA011	pEX18.Ap PABL049 ΔAGEv5::Gmr; oligos29, 30, 31, 32,163, 164; PABL049 GenDNA, pJA001	This Study
pJA012	pEX18.Ap PABL012 ΔAGEv6::Gmr; oligos33, 34, 35, 36,163, 164; PABL012 GenDNA, pJA001	This Study
pJA013	pEX18.Ap PABL049 ΔAGEv6::Gmr; oligos37, 38, 39, 40,163, 164; PABL049 GenDNA, pJA001	This Study
pJA014	pEX18.Ap PABL012 ΔAGEv7::Gmr; oligos41, 42, 43, 44,163, 164; PABL012 GenDNA, pJA001	This Study
pJA015	pEX18.Ap PABL049 ΔAGEv7::Gmr; oligos45, 46, 47, 48,163, 164; PABL049 GenDNA, pJA001	This Study
pJA016	pEX18.Ap PABL016 ΔAGEv8::Gmr; oligos49, 50, 51, 52,163, 164; PABL016 GenDNA, pJA001	This Study
pJA017	pEX18.Ap PABL012 ΔAGEv9::Gmr; oligos53, 54, 55, 56,163, 164; PABL012 GenDNA, pJA001	This Study
pJA018	pEX18.Ap PABL049 ΔAGEv9::Gmr; oligos57, 58, 59, 60,163, 164; PABL049 GenDNA, pJA001	This Study
pJA019	pEX18.Ap PABL016 ΔAGEv10::Gmr; oligos61, 62, 63, 64,163, 164; PABL016 GenDNA, pJA001	This Study
pJA020	pEX18.Ap PABL012 ΔAGEv11::Gmr, oligos200, 201, 202, 203, 163, 164; PABL012 GenDNA, pJA001	This Study
pJA022	pEX18.Ap PABL012 ΔAGEv12::Gmr; oligos73, 74, 75, 76,163, 164; PABL012 GenDNA, pJA001	This Study
pJA023	pEX18.Ap PABL049 ΔAGEv12::Gmr; oligos77, 78, 79, olgio80,163, 164; PABL049 GenDNA, pJA001	This Study
pJA024	pEX18.Ap PABL083 ΔAGEv13::Gmr; oligos81, 82, 83, 84,163, 164; PABL083 GenDNA, pJA001	This Study
pJA025	pEX18.Ap PABL107 ΔAGEv13::Gmr; oligos85, olgio86, 87, 88,163, 164; PABL107 GenDNA, pJA001	This Study
pJA026	pEX18.Ap PABL012 ΔAGEv14::Gmr; oligos89, 90, 91, 92,163, 164; PABL012 GenDNA, pJA001	This Study
pJA027	pEX18.Ap PABL017 ΔAGEv15::Gmr; oligos93, 94, 95, 96,163, 164; PABL017 GenDNA, pJA001	This Study
pJA028	pEX18.Ap PABL012 ΔAGEx1::Gmr; oligos97, 98, 99, 100; PABL012 GenDNA, pJA001	This Study
pJA029	pEX18.Ap PABL012 ΔAGEx2::Gmr; oligos101, 102, 103, 104; PABL012 GenDNA, pJA001	This Study
pJA030	pEX18.Ap PABL016 ΔAGEx3::Gmr; oligos105, 106, 107, 108; PABL016 GenDNA, pJA001	This Study
pJA031	pEX18.Ap PABL012 ΔAGEx4::Gmr; oligos109, 110, 111, 112; PABL012 GenDNA, pJA001	This Study
pJA032	pEX18.Ap PABL049 ΔAGEx5::Gmr; oligos113, 114, 115, 116; PABL049 GenDNA, pJA001	This Study
pJA034	pEX18.AP Cdi1AΔCT ^{PABL017}::Gmr; oligos121, 122, 123, 124,163, 164; PABL017 GenDNA, pJA001	This Study
pJA035	pMCSG53_Cdi1A-CT[3108]^{PABL017} /CdiI^{PABL017}; oligos 159, 158; PABL017 GenDNA	This Study
pJA036	pMCSG53_Cdi1A-CT[3345]^{PABL017} /CdiI^{PABL017}; oligos155, 158; PABL017 GenDNA	This Study
pJA037	pMCSG53_Cdi1A-CT[3345](H3372A)^{PABL017}/CdiI^{PABL017}; oligos155, 158, 173, 174; PABL017 GenDNA	This Study
pJA038	pMCSG53_Cdi1I-ST ^{PABL017}; oligos157, 160; PABL017 GenDNA	This Study
pJA039	pEX18.GM Cdi1AΔCT ^{PABL017}; oligos129, 130, 131, 132; PABL017 GenDNA	This Study
pJA040	pEX18.GM Cdi1AΔCT/I ^{PABL017}; oligos133, 134, 135, 136; PABL017 GenDNA	This Study
pJA041	pEX18.GM Cdi1A(H3372A) ^{PABL017}; oligos125, 126, 127, olgio128; PABL017 GenDNA	This Study
pJA042	pEX18.GM Cdi1AΔCTcomp ^{PABL017}; oligos141, 142; PABL017 GenDNA	This Study
pJA043	pEX18.GM Cdi1AΔCTIcomp ^{PABL017}; oligos141, 140; PABL017 GenDNA	This Study
pJA044	pEF1α Cdi1A-CT[3345]^{PABL017}/CdiI ^{PABL017}-IRES-AcGFP1A ; oligos151,154; PABL017 GenDNA	This Study
pJA045	pEF1α Cdi1A-CT[3345](H3372A)^{PABL017}-IRES-AcGFP1A ; oligos151, 152; PABL017 GenDNA	This Study
pJA046	pEF1α CdiI^{PABL017}-IRES-AcGFP1A ; oligos153, 154; PABL017 GenDNA	This Study
pJA047	pEX18.GM PABL017Δ*dppBC*; oligos145, 146, 147, olgio148; PABL017 GenDNA	This Study

Apr = Ampicillin resistance, Gmr = Gentamicin resistance, Kanr = Kanamycin resistance, Neor = Neomycin resistance

Table S3. List of oligonucleotides.

Oligo	Relevant characteristic	Sequence (5'-3')
oligo001	pEX18_PABL12ΔAGEv1_Fdn	AAGATCCCCAATTCGCTGCAGCAGCTAAATGGTCGAAA
oligo002	pEX18_PABL12ΔAGEv1_Fup	GCTCTAGAGCCTTTAGTGAAATAGCTTGG
oligo003	pEX18_PABL12ΔAGEv1_Rdn	GCTCTAGAGCACAGACCCACAACAGGTA
oligo004	pEX18_PABL12ΔAGEv1_Rup	AGAGCGCTTTTGAAGCTAATATCAATAGACCTCCCTCC
oligo005	pEX18_PABL26ΔAGEv2_Fdn	AAGATCCCCAATTCGCTGCACAGCAGCAGTTCCCGCGCCT
oligo006	pEX18_PABL26ΔAGEv2_Fup	GCTCTAGAGCATACAAGTCCCTTGGTGA
oligo007	pEX18_PABL26ΔAGEv2_Rdn	GCTCTAGAGCTCAGGACTTTCCTCCGAG
oligo008	pEX18_PABL26ΔAGEv2_Rup	AGAGCGCTTTTGAAGCTAATATAGTTACGCCCTGGTAG
oligo013	pEX18_PABL49ΔAGEv2_Fdn	AAGATCCCCAATTCGCTGCATCGACGCGGCAGCTTGATCCCAG
oligo014	pEX18_PABL49ΔAGEv2_Fup	GCTCTAGAGCAGACGGATTCCAGAAAAG
oligo015	pEX18_PABL49ΔAGEv2_Rdn	GCTCTAGAGCTGTAAGGCCGTACCTGCAC
oligo016	pEX18_PABL49ΔAGEv2_Rup	AGAGCGCTTTTGAAGCTAATAGATCCACCAGCCATCAC
oligo017	pEX18_PABL16ΔAGEv3_Fdn	AAGATCCCCAATTCGCTGCACGAGATCACCCTGGCGCA
oligo018	pEX18_PABL16ΔAGEv3_Fup	GCTCTAGAGCTGGTACCGAAGGAAAATG
oligo019	pEX18_PABL16ΔAGEv3_Rdn	GCTCTAGAGCATCGAGATGGGCATTGGCGCAG
oligo020	pEX18_PABL16ΔAGEv3_Rup	AGAGCGCTTTTGAAGCTAATTGCGGCTGGCGGAACGGT
oligo025	pEX18_PABL7ΔAGEv4_Fdn	AAGATCCCCAATTCGCTGCATAAAAAAATCCAGCCACC
oligo026	pEX18_PABL7ΔAGEv4_Fup	GCTCTAGAGCAGCAAATTCTGCCGGGGTGAGA
oligo027	pEX18_PABL7ΔAGEv4_Rdn	GCTCTAGAGCTATTATCAGCGCCAGGAC
oligo028	pEX18_PABL7ΔAGEv4_Rup	AGAGCGCTTTTGAAGCTAATCCTCAAGCAGGCGGAGGCCGGTG
oligo029	pEX18_PABL49ΔAGEv5_Fdn	AAGATCCCCAATTCGCTGCAAGGGTCGCAGTTCGAACAGC
oligo030	pEX18_PABL49ΔAGEv5_Fup	GCTCTAGAGCGAAGAAACTGCTGAAGTT
oligo031	pEX18_PABL49ΔAGEv5_Rdn	GCTCTAGAGCCGTCCATCGAACGCGCGC
oligo032	pEX18_PABL49ΔAGEv5_Rup	AGAGCGCTTTTGAAGCTAATTTCCAGCAGGTTGTCGAT
oligo033	pEX18_PABL12ΔAGEv6.Fup	GCTCTAGAGCGCACAAAACCCTTCCGCCCGCC
oligo034	pEX18_PABL12ΔAGEv6.Rup	AGAGCGCTTTTGAAGCTAATCTGGCGCTGGTCGGGAAAATTC
oligo035	pEX18_PABL12ΔAGEv6.Fdn	AAGATCCCCAATTCGCTGCAACCGACCTCTCCCAGCACACGCCGAT
oligo036	pEX18_PABL12ΔAGEv6.Rdn	GCTCTAGAGCGGTTTCCCAGCCTTTTATCTCCTG
oligo037	pEX18_PABL49ΔAGEv6.Fup	GCTCTAGAGCCAGCAGGGTTTCCCAGCCTTTT
oligo038	pEX18_PABL49ΔAGEv6.Rup	AGAGCGCTTTTGAAGCTAATACACACGCCGATGATGCAGCAG
oligo039	pEX18_PABL49ΔAGEv6.Fdn	AAGATCCCCAATTCGCTGCATCATGGGCAATACCTCCCCGTCCTGCTGG
oligo040	pEX18_PABL49ΔAGEv6.Rdn	GCTCTAGAGCATGAGATCGCCGGCCTCCGCTACTA
oligo041	pEX18_PABL12ΔAGEv7.Fup	GCTCTAGAGCGAGGCTTTGCTCGATGAGCAGC
oligo042	pEX18_PABL12ΔAGEv7.Rup	AGAGCGCTTTTGAAGCTAATCATATGCGCCCAGTGTCTCAGC
oligo043	pEX18_PABL12ΔAGEv7.Fdn	AAGATCCCCAATTCGCTGCAGGTTCAACAGTTCCAGCGGGCA
oligo044	pEX18_PABL12ΔAGEv7.Rdn	GCTCTAGAGCGGCAGATTGAAGGTGACAAACT
oligo045	pEX18_PABL49ΔAGEv7.Fup	GCTCTAGAGCGAGGCTTTGCTCGATGAGCAGC
oligo046	pEX18_PABL49ΔAGEv7.Rup	AGAGCGCTTTTGAAGCTAATCATATGCGCCCAGTGTCTCAGC
oligo047	pEX18_PABL49ΔAGEv7.Fdn	AAGATCCCCAATTCGCTGCAGGTTCAACAGTTCCAGCGGGCA
oligo048	pEX18_PABL49ΔAGEv7.Rdn	GCTCTAGAGCAATCCATGACCACCAGGGGCTG
oligo049	pEX18_PABL16ΔAGEv8.Fup	GCTCTAGAGCCTGGATGATGTCGTTAGACTTTCTCAAA
oligo050	pEX18_PABL16ΔAGEv8.Rup	AGAGCGCTTTTGAAGCTAATGGAAAAAGGGGACAGATTTATTTT
oligo051	pEX18_PABL16ΔAGEv8.Fdn	AAGATCCCCAATTCGCTGCAAAGAGGGTTTCCTCCTACATAG
oligo052	pEX18_PABL16ΔAGEv8.Rdn	GCTCTAGAGCAACGCATCGTCAAGCTCACCCC
oligo053	pEX18_PABL12ΔAGEv9.Fup	GCTCTAGAGCAGGACGTCGGCGATGATCTCGT
oligo054	pEX18_PABL12ΔAGEv9.Rup	AGAGCGCTTTTGAAGCTAATGGCAACATCCCCAGCAGCGGCT
oligo055	pEX18_PABL12ΔAGEv9.Fdn	AAGATCCCCAATTCGCTGCATCGATCTTCATCACTTTGGTTT
oligo056	pEX18_PABL12ΔAGEv9.Rdn	GCTCTAGAGCATCGCTACGAGGCGCGTATCTG
oligo057	pEX18_PABL49ΔAGEv9.Fup	GCTCTAGAGCAGGACGTCGGCGATGATCTCGT
oligo058	pEX18_PABL49ΔAGEv9.Rup	AGAGCGCTTTTGAAGCTAATGGCAACATCCCCAGCAGCGGCT
oligo059	pEX18_PABL49ΔAGEv9.Fdn	AAGATCCCCAATTCGCTGCACACCTTGGTTTCGGCAGTGAGC
oligo060	pEX18_PABL49ΔAGEv9.Rdn	GCTCTAGAGCGCTACGAGGCGCGCATCTGGGC
oligo061	pEX18_PABL16ΔAGEv10.Fup	GCTCTAGAGCGCCATCCGCCAGTGCGCCATGC
oligo062	pEX18_PABL16ΔAGEv10.Rup	AGAGCGCTTTTGAAGCTAATTCCGCCAGCCGGTGCCTGTTTT
oligo063	pEX18_PABL16ΔAGEv10.Fdn	AAGATCCCCAATTCGCTGCAGGCCAGTGATCGGCGATCCGGTACCA
oligo064	pEX18_PABL16ΔAGEv10.Rdn	GCTCTAGAGCTAGCAGACATCGACGCCAGCACCGACA
oligo065	pEX18_PABL13ΔAGEv14.Fup	GCTCTAGAGCTTCGAGACTTACCGCACCGACG
oligo066	pEX18_PABL13ΔAGEv14.Rup	AGAGCGCTTTTGAAGCTAATGTTCTCGCGGAGACGATCCACC
oligo067	pEX18_PABL13ΔAGEv14.Fdn	AAGATCCCCAATTCGCTGCAAATGTATGGACGATTCGTCAAC
oligo068	pEX18_PABL13ΔAGEv14.Rdn	GCTCTAGAGCACACATACCCGGGAACCCCCAT
oligo073	pEX18_PABL12ΔAGEv12.Fup	GCTCTAGAGCGGCGATAACGGTGAGCTTCCGA
oligo074	pEX18_PABL12ΔAGEv12.Rup	AGAGCGCTTTTGAAGCTAATCCAGAGCGCCCAGGCGTAATCG
oligo075	pEX18_PABL12ΔAGEv12.Fdn	AAGATCCCCAATTCGCTGCATCGAAAGGGACTTGCAGAGCGA
oligo076	pEX18_PABL12ΔAGEv12.Fup	GCTCTAGAGCTGCAGCGACTGGAGCTTCTTGTC
oligo077	pEX18_PABL49ΔAGEv12.Fup	GCTCTAGAGCGCGCCACGTTCAGCCGGTTCGC
oligo078	pEX18_PABL49ΔAGEv12.Rup	AGAGCGCTTTTGAAGCTAATCCAGAGCGCCCAGGCGTATTCG
oligo079	pEX18_PABL49ΔAGEv12.Fdn	AAGATCCCCAATTCGCTGCACGAAAGGGACTTGCAGAGCGAT

oligo080	pEX18_PABL49ΔAGEv12.Rdn	GCTCTAGAGCTGCAGCGACTGGAGCTTCTTGTC
oligo081	pEX18_PABL83ΔAGEv13.Fup	GCTCTAGAGCGCAGCATGATGTCCAGCAGGAT
oligo082	pEX18_PABL83ΔAGEv13.Rup	AGAGCGCTTTTGAAGCTAATAAACGAAAGGCACCCGCACTCT
oligo083	pEX18_PABL83ΔAGEv13.Fdn	AAGATCCCCAATTCGCTGCACGCTGGCTACTTGAGCACCTTG
oligo084	pEX18_PABL83ΔAGEv13.Rdn	GCTCTAGAGCCAAGGGCACCCTGCTGCTGGCG
oligo085	pEX18_PABL107ΔAGEv13.Fup	GCTCTAGAGCGCAGCATGATGTCCAGCAGGAT
oligo086	pEX18_PABL107ΔAGEv13.Rup	AGAGCGCTTTTGAAGCTAATAAACGAAAGGCACCCGCACTCT
oligo087	pEX18_PABL107ΔAGEv13.Fdn	AAGATCCCCAATTCGCTGCACGCTGGCTACTTGAGCACCTTG
oligo088	pEX18_PABL107ΔAGEv13.Rdn	GCTCTAGAGCCAAGGGCACCCTGCTGCTGGCG
oligo089	pEX18_PABL12ΔAGEv14.Fup	GCTCTAGAGCGGCGATAACGGTGAGCTTCCGA
oligo090	pEX18_PABL12ΔAGEv14.Rup	AGAGCGCTTTTGAAGCTAATTACTTCGAGGATAACGCCGCGC
oligo091	pEX18_PABL12ΔAGEv14.Fdn	AAGATCCCCAATTCGCTGCATGTCGGCAGTGCTTCGGAAGCGCCGCCAT GATCAC
oligo092	pEX18_PABL12ΔAGEv14.Rdn	GCTCTAGAGCTCGAGGAGGCTGGTGTGATTCG
oligo093	pEX18_PABL17ΔAGEv15.Fup	TCCCCCCGGGGGGACAGGCGGAGGGTCGGCTGGCAC
oligo094	pEX18_PABL17ΔAGEv15.Rup	AGAGCGCTTTTGAAGCTAATTCTGGCCCTGGCGGTCCTCGACGGC
oligo095	pEX18_PABL17ΔAGEv15.Fdn	ATTGACTGATGAAAGAATTATTTGAAGTG
Oligo096	pEX18_PABL17ΔAGEv15.Rdn	TCCCCCCGGGGGGATAAAAAACCTAGTC
Oligo097	pEX18_PABL12ΔAGEx1_Fdn	AAGATCCCCAATTCGCTGCAAAGGTCGAGAAGATCACGGCTG
Oligo098	pEX18_PABL12ΔAGEx1_Fup	TCCCCCCGGGGGGACCAGTGGAAAGGGAAATCACATGGAA
Oligo099	pEX18_PABL12ΔAGEx1_Rdn	TCCCCCCGGGGGGATATTGCCGTTGGGATCGATGGAACTGAT
oligo100	pEX18_PABL12ΔAGEx1_Rup	AGAGCGCTTTTGAAGCTAATCTCCCGGTAGCTGAGACGAGATTTGGC
oligo101	pEX18_PABL12ΔAGEx2_Fdn	AAGATCCCCAATTCGCTGCATCGGCGCGCTGCGGCGTTACCTGGAAA
oligo102	pEX18_PABL12ΔAGEx2_Fup	TCCCCCCGGGGGGAGATACTCCGGAAAAAGAGCAGGCAACAT
oligo103	pEX18_PABL12ΔAGEx2_Rdn	TCCCCCCGGGGGGAGGAGCTGGCCGTTTCGGTACGC
oligo104	pEX18_PABL12ΔAGEx2_Rup	AGAGCGCTTTTGAAGCTAATGGCCTGCGGGCCTTTGGCGCCTGCGGTA
oligo105	pEX18_PABL16ΔAGEx3_Fdn	AAGATCCCCAATTCGCTGCAGATCCGCGTGCGCAGGCTTTCGTGC
oligo106	pEX18_PABL16ΔAGEx3_Fup	TCCCCCCGGGGGGAGCTCGCGCGGGTATTCGATGTC
oligo107	pEX18_PABL16ΔAGEx3_Rdn	TCCCCCCGGGGGGAAGCGAGGTCGGCGTGGAGCTGC
oligo108	pEX18_PABL16ΔAGEx3_Rup	AGAGCGCTTTTGAAGCTAATTCTATGCGACCGATCTATTCGA
oligo109	pEX18_PABL12ΔAGEx4_Fdn	AAGACCCCAATTCGCTGCACCGTGTGGACCATGGGAATAGC
oligo110	pEX18_PABL12ΔAGEx4_Fup	TCCCCCCGGGGGGAATGTCCTTGCCAGCGTCTAGCC
oligo111	pEX18_PABL12ΔAGEx4_Rdn	TCCCCCCGGGGGGAGCAAGCCAAATAAAAGGTTTAC
oligo112	pEX18_PABL12ΔAGEx4_Rup	AGAGCGCTTTTGAAGCTAATTGCCGATCTGCCTATAAGTGAT
oligo113	pEX18_PABL49ΔAGEx5_Fdn	AAGATCCCCAATTCGCTGCAGTATCGACGACGATATCGCCTATCCGTA
oligo114	pEX18_PABL49ΔAGEx5_Fup	TCCCCCCGGGGGGAGACAGTCTGAGTCAGGGCTGCC
oligo115	pEX18_PABL49ΔAGEx5_Rdn	TCCCCCCGGGGGGATACAAGGATGAATTCTCGATGGGAAGCG
oligo116	pEX18_PABL49ΔAGEx5_Rup	AGAGCGCTTTTGAAGCTAATTTCTTCTACGAGGAGTGGAGAA
oligo121	pEX18_PABL17CdiAΔCT_Fup	TCCCCCCGGGGGGACAGGCCACGGTGT
oligo122	pEX18_PABL17CdiAΔCT_Rup	AAGATCCCCAATTCGCTGCATGAAAGAA
oligo123	pEX18_PABL17CdiAΔCT_Fdn	TCCCCCCGGGGGGATATGCTCCTAAAGA
oligo124	pEX18_PABL17CdiAΔCT_Rdn	AGAGCGCTTTTGAAGCTAATGGACGCAT
oligo125	pEX18_H3372A_Fup	CGGGTACCGAGCTCGGATCTCTTTGCCCTGGACAAGC
oligo126	pEX18_H3372A_Rup	TGCCTACCCGCAGCTTTAGATAGCGCATGTCC
oligo127	pEX18_H3372A_Fdn	GGACATGCGCTATCTAAAGCTGCGGGTAGGCA
oligo128	pEX18_H3372A_Rdn	ATGACCATGATTACGCTAAAGAAGAGGACCCAGCCTGTT
oligo129	pEX18_BL017_CdiAΔCT_Fup	CGGGTACCGAGCTCGCCGAGCGTTCAAACGCTATC
oligo130	pEX18_BL017_CdiAΔCT_Rup	AATAAACCCTTTAAAAGTAGCGTTCGATCCAACAC
oligo131	pEX18_BL017_CdiAΔCT_Fdn	GAACGCTACTTTTAAAGGGTTTATTGACTGATGAA
oligo132	pEX18_BL017_CdiAΔCT_Rdn	ATGACCATGATTACGACGCTCAAAGCAAATAATTC
oligo133	pEX18_BL017_CdiAΔCTl_Fup	CGGGTACCGAGCTCGAGGATTGTCGCGCGGCAGGC
oligo134	pEX18_BL017_CdiAΔCTl_Rup	ATTTTTTATGCTCTCAAGTAGCGTTCGATCCAACAC
oligo135	pEX18_BL017_CdAΔCTl_Fdn	GGATCGAACGCTACTTGAGAGCATAAAAAATAAAATAAAGGGACCAG
oligo140	pEX18_BL017_CdiAΔCTl_Rdn	ATGACCATGATTACGCATCTTCGAATCTTGCCATC
oligo141	pEX18_BL017_CdiA-CT_Comp_F	CGGGTACCGAGCTCGGCAGCCCTGGCTGCTGGCGCCAACG
oligo142	pEX18_BL017_CdiA-CT_Comp_R	ATGACCATGATTACGAAACCACTCGCCCTTGCCTAGGCATC
oligo143	p53_BL017_CdiA-CT_F	TACTTCCAATCCAATTTTGGTCAAATTAAAACAGTG
oligo144	p53_BL017_CdiA-CT_R	TTATCCACTTCCAATTCAGTCAATAAACCCTTTAAAAG
oligo145	pEX18_PABL017 dppBC_Fup	CCGGGTACCGAGCTCGTCAACACCCAGCACAAGCCGCTCGA
oligo146	pEX18_PABL017 dppBC_Rup	GGTTGTGCTCCTCATGCAAGCATGTTGGCGGGTAACTCCTCATCGCG
oligo147	pEX18_PABL017 dppBC_Fdn	TACCCGCCAACATGCTTGCATGAGGAGCACAACCATGAACAGCGCAT
oligo148	pEX18_PABL017 dppBC_Rdn	CTATGACCATGATTACGTTGATCAGCGCCTCGGTGTAGGGATG
oligo151	pEF1alpha_BL017_CT_F	CGAGCTCAAGCTTCGTTTGGTCAAATTAAAACAGTGCTTG
oligo152	pEF1alpha_BL017_CT_R	GTACCGTCGACTGCAGTCAGTCAATAAACCCTTTAAAAG
oligo153	pEF1alpha_BL017_CdiI_F	CGAGCTCAAGCTTCGATGAAAGAATTATTTGAAGTG
oligo154	pEF1alpha_BL017_CdiI_R	GTACCGTCGACTGCAGCTAAAGAAGAGGACCCAGCCTG
oligo155	p53_BL017_CdiA-CT_F	TTATCCACTTCCAATTTTGGTCAAATTAAAACAGTG
oligo156	p53_BL017_CdiA-CT_R	TACTTCCAATCCAATTCAGTCAATAAACCCTTTAAAAG
oligo157	P53_BL017_CdiI_F	TTAAGAAGGAGATATACAATGAAAGAATTATTTGAAGTGATTTTTGAGG
oligo158	p53_BL017_CdiI_R	TTATCCACTTCCAATGCTAAAGAAGAGGACCCAGCCTGTTG

oligo159	p53_BL017_CdiA-CT(3108)_F	TACTTCCAATCCAATGCGCTCGTCGGTGAAAAGATCTTC
oligo160	p53_BL017_CdiI-ST_R	ACTGCAGCTATTTTTCGAACTGCGGGTGGCTCCAAAGAAGAGGACCCAG CCTGTTG
oligo161	pCTX_F-BamHI	CGGGATCCCGTGCTGTTGACAAAGGGAATC
oligo162	pCTX_R-EcoRI	CGGAATTCCGAGCACATCAGCTTCAAAAGC
oligo163	Gm-pCTX_F-BamHI	CGGGATCCCGCCGCTCATGAGACAATAACCCTGA
oligo164	Gm-pCTX_R-EcoRI	CGGAATTCCGAAAGTATATATGAGTAAACTT
oligo165	Gm_FFC_F	ATTAGCTTCAAAAGCGCTCT
oligo166	Gm_FFC_R	TGCAGCGAATTGGGGATCTT
oligo167	pJPA1.pBAD_F-KpnI	GGGGTACCTTATGACAACTTGACGGCTACATC
oligo168	pJPA1.pBAD.MCS_R-HindIII	CCCAAGCTTGCATGCCTGCAGGTCGACTCTAGAGGATCCCCGGGTATAT CTCCTTCTTAG
oligo169	pJPA1_CdiI^{PABL17}_F	GCTCTAGAATGAAAGAATTATTTGAAGTGATTTTTG
oligo170	pJPA1_CdiI^{PABL17}_R	AACTGCAGCTAAAGAAGAGGACCCAGCCTGTTG
oligo171	pBADpro_F(MC)	GCTGCAGGAATTCGATATCATTATGACAACTTGACGGCTACATCATTCAC
oligo172	CdiI^{PABL17}_R(MC)	AGGTCGACGGTATCGATACTAAAGAAGAGGACCCAGCCTGTTGTTAG
oligo173	H3372A_F	GCGCTATCTAAAGCTGCGGGTAGGCATCCC
oligo174	H3372A_R	GGGATGCCTACCCGCAGCTTTAGATAGCGC
oligo175	TnMut_Round1_PA	GGCCACGCGTCGACTAGTAGnnnnnnnnnCAGCAG
oligo176	TnMut_Round1_pBT20	AGACCGGGGACTTATCAGCCAACCTGTTA
oligo177	TnMut_Round2_PA	GGCCACGCGTCGACTAGTAC
oligo178	TnMut_Round2_pBT20	CGCACTCCCGTTCTGGATAATGTT
oligo179	Illumina_Tn_Ad1	TCGTCGGCAGCGTCAGATGTGTATAAGAGACAGCGCACTCCCGTTCTGG ATAATGTT
oligo180	Illumina_Tn_Ad2	GTCTCGTGGGCTCGGAGATGTGTATAAGAGACAGGGCCACGCGTCGAC TAGTAC
oligo181	PA-Ala	/5Biosg/AAGCAGGCGCTCTCCCAGCTG
oligo182	PA-Arg-ACG	/5Biosg/AGCCGAGTACTCTATCCAGCT
oligo183	PA-Cys	/5Biosg/AATCCGGTGCATAACCACTCT
oligo184	PA-Gln	/5Biosg/AACCTGCTGCCTTACCGCTTG
oligo185	PA-Glu	/5Biosg/AGGGCGGTGTCCTAGGCCACT
oligo186	PA-Leu(CAA)	/5Biosg/AATCCGCCGCGTCTACCGATT
oligo187	PA-Pro-CGG	/5Biosg/AACGAGACGCGCTACCAAGCT
oligo188	PA-Ser-CGA	/5Biosg/AATCCGTCCCGTTCGACCACT
oligo189	PA-Trp	/5Biosg/AGACCGCCGCTCTGCCAATTG
oligo190	PA-Tyr	/5Biosg/AGTCTGATCCCTTTGGCCACT
oligo191	Hu-Gln-1	/5Biosg/CAGAGTCCAGAGTGCTAACCATTACACCATGGA
oligo192	Hu-Gln-2	/5Biosg/CAGAGTCCAGAGTGCTTACCATTACACCATGGA
oligo193	Hu-Gln-3	/5Biosg/CAGAGTCCAGAGTGCTCACCATTACACCATGGA
oligo194	Hu-Pro-1	/5Biosg/CCGAAGCGAGAATCATACCCCTAGACCAACGAGCC
oligo195	Hu-Pro-2	/5Biosg/CCAAAGCGAGAATCATACCCCTAGACCAACGAGCC
oligo196	Hu-Pro-3	/5Biosg/CCTAAGCGAGAATCATACCCCTAGACCAACGAGCC
oligo197	Hu-Pro-5	/5Biosg/CTCGTCCGGGATTTGAACCCGGGACCTCTCGC
oligo198	Hu-Gly-1	/5Biosg/GGCAGGCGAGAATTCTACCACTGAACCACCAA
oligo199	Hu-Gly-2	/5Biosg/GCCGGGAATCGAACCCGGGCCTCCCGCG
oligo200	pEX18_PABL012ΔAGEv11.Fup	TCGAGACTTACCGCACCGATGG
oligo201	pEX18_PABL012ΔAGEv11.Rup	AGAGCGCTTTTGAAGCTAATGTTCTCGCGGAGACGATCCACC
oligo202	pEX18_PABL012ΔAGEv11.Fdn	AAGATCCCCAATTCGCTGCACATGTACGGACGATTCGTCAAC
oligo203	pEX18_PABL012ΔAGEv11.Rdn	TCTGCTTCGCCGTGTTGTCGAT

Table S4. Crystallization information.

Method	Vapor diffusion, sitting drop
Plate type	96-well microplate
Temperature (˚C)	19
Protein concentration (mg ml^{-1})	6.4
Protein solution	500 mM Sodium chloride, 10 mM Tris-HCl pH 8.3, 5 mM BME
Reservoir Solution	100 mM Bis-Tris pH 6.5, 25% (w/v) PEG 3350
Volume and ratio of drop	1 µl :1 µl
Volume of reservoir (µl)	100

Table S5. Crystallization data collection and processing.

Diffraction source	Beamline 21-ID-F, APS
Wavelength (Å)	0.97872
Temperature (K)	100
Detector	MAR Mosaic 300 mm CCD
Space group	$P6_3$
a,b,c (Å)	76.58, 76.58, 61.44
α, β, γ (°)	90.00, 90.00, 120.00
Resolution range (Å)	30.00 – 1.75 (1.78 – 1.75)
No. of unique reflections	20855 (1035)
Completeness (%)	99.9 (100.0)
Multiplicity	6.6 (6.6)
$\langle I/\sigma(I) \rangle$	30.7 (2.4)
R_{merge}	0.075 (0.799)
$R_{r.i.m.}$ ‡	0.032 (0.340)
$CC_{1/2}$ ‡‡	(0.722)
Overall B factor from Wilson Plot (Å^2)	25.1

Table S6. Crystal structure refinement.

Resolution range (Å)	29.18 – 1.75 (1.795 – 1.750)
Completeness (%)	99.9 (100.0)
No. of reflections, working set	19733 (1442)
No. of reflections, test set	1012 (85)
Final R_{work}	0.183 (0.288)
Final R_{free}	0.224 (0.280)
No. of non-H atoms	
Protein	2014
Water	105
Total	2119
R.m.s. deviations	
Bonds (Å)	0.009
Angles (°)	1.507
Average B factors (Å^2)	
Protein	38.3
Water	33.7
Ramachandran plot[‡]	
Favored regions (%)	96.0
Additionally allowed (%)	4.0
Outliers (%)	0.0

Values in parenthesis are for outer shell

SI References

1. E. A. Ozer, J. P. Allen, A. R. Hauser, Characterization of the core and accessory genomes of Pseudomonas aeruginosa using bioinformatic tools Spine and AGEnt. *BMC Genomics* **15**, 737 (2014).
2. E. A. Ozer, ClustAGE: a tool for clustering and distribution analysis of bacterial accessory genomic elements. *BMC Bioinformatics* **19**, 150 (2018).
3. G. H. Van Domselaar *et al.*, BASys: a web server for automated bacterial genome annotation. *Nucleic Acids Res* **33**, W455-459 (2005).
4. K. Rutherford *et al.*, Artemis: sequence visualization and annotation. *Bioinformatics* **16**, 944-945 (2000).
5. D. Arndt *et al.*, PHASTER: a better, faster version of the PHAST phage search tool. *Nucleic Acids Res* **44**, W16-21 (2016).
6. M. J. Sullivan, N. K. Petty, S. A. Beatson, Easyfig: a genome comparison visualizer. *Bioinformatics* **27**, 1009-1010 (2011).
7. T. T. Hoang, A. J. Kutchma, A. Becher, H. P. Schweizer, Integration-proficient plasmids for Pseudomonas aeruginosa: site-specific integration and use for engineering of reporter and expression strains. *Plasmid* **43**, 59-72 (2000).
8. T. T. Hoang, R. R. Karkhoff-Schweizer, A. J. Kutchma, H. P. Schweizer, A broad-host-range Flp-FRT recombination system for site-specific excision of chromosomally-located DNA sequences: application for isolation of unmarked Pseudomonas aeruginosa mutants. *Gene* **212**, 77-86 (1998).
9. K. H. Choi, A. Kumar, H. P. Schweizer, A 10-min method for preparation of highly electrocompetent Pseudomonas aeruginosa cells: application for DNA fragment transfer between chromosomes and plasmid transformation. *J Microbiol Methods* **64**, 391-397 (2006).
10. H. P. Schweizer, T. T. Hoang, An improved system for gene replacement and xylE fusion analysis in Pseudomonas aeruginosa. *Gene* **158**, 15-22 (1995).
11. R. Simon, U. Priefer, A. Puhler, A Broad Host Range Mobilization System for In Vivo Genetic Engineering: Transposon Mutagenesis in Gram Negative Bacteria. *Bio/Technology* **1**, 784-791.
12. W. H. Eschenfeldt *et al.*, New LIC vectors for production of proteins from genes containing rare codons. *J Struct Funct Genomics* **14**, 135-144 (2013).
13. T. G. Schmidt, J. Koepke, R. Frank, A. Skerra, Molecular interaction between the Strep-tag affinity peptide and its cognate target, streptavidin. *J Mol Biol* **255**, 753-766 (1996).
14. A. M. Bolger, M. Lohse, B. Usadel, Trimmomatic: a flexible trimmer for Illumina sequence data. *Bioinformatics* **30**, 2114-2120 (2014).
15. J. G. Caporaso *et al.*, QIIME allows analysis of high-throughput community sequencing data. *Nat Methods* **7**, 335-336 (2010).
16. S. F. Altschul, W. Gish, W. Miller, E. W. Myers, D. J. Lipman, Basic local alignment search tool. *J Mol Biol* **215**, 403-410 (1990).
17. M. L. Kuhn, K. A. Majorek, W. Minor, W. F. Anderson, Broad-substrate screen as a tool to identify substrates for bacterial Gcn5-related N-acetyltransferases with unknown substrate specificity. *Protein science : a publication of the Protein Society* **22**, 222-230 (2013).
18. L. Shuvalova, Parallel protein purification. *Methods Mol Biol* **1140**, 137-143 (2014).
19. W. Minor, M. Cymborowski, Z. Otwinowski, M. Chruszcz, HKL-3000: the integration of data reduction and structure solution--from diffraction images to an initial model in minutes. *Acta Crystallogr D Biol Crystallogr* **62**, 859-866 (2006).
20. G. N. Murshudov, A. A. Vagin, E. J. Dodson, Refinement of macromolecular structures by the maximum-likelihood method. *Acta Crystallogr D Biol Crystallogr* **53**, 240-255 (1997).
21. P. Emsley, K. Cowtan, Coot: model-building tools for molecular graphics. *Acta Crystallogr D Biol Crystallogr* **60**, 2126-2132 (2004).
22. M. D. Winn *et al.*, Overview of the CCP4 suite and current developments. *Acta Crystallogr D Biol Crystallogr* **67**, 235-242 (2011).
23. R. J. Morris, A. Perrakis, V. S. Lamzin, ARP/wARP and automatic interpretation of protein electron density maps. *Methods Enzymol* **374**, 229-244 (2003).

24. J. Painter, E. A. Merritt, Optimal description of a protein structure in terms of multiple groups undergoing TLS motion. *Acta Crystallogr D Biol Crystallogr* **62**, 439-450 (2006).
25. V. B. Chen *et al.*, MolProbity: all-atom structure validation for macromolecular crystallography. *Acta Crystallogr D Biol Crystallogr* **66**, 12-21 (2010).
26. L. Holm, L. M. Laakso, Dali server update. *Nucleic Acids Res* **44**, W351-355 (2016).
27. E. L. Kaplan, P. Meier, Nonparametric Estimation from Incomplete Observations. *Journal of the American Statistical Association* **53**, 457-481 (1958).
28. N. Mantel, Evaluation of survival data and two new rank order statistics arising in its consideration. *Cancer Chemother Rep* **50**, 163-170 (1966).
29. C. M. Shaver, A. R. Hauser, Relative contributions of *Pseudomonas aeruginosa* ExoU, ExoS, and ExoT to virulence in the lung. *Infect Immun* **72**, 6969-6977 (2004).
30. C. A. Schneider, W. S. Rasband, K. W. Eliceiri, NIH Image to ImageJ: 25 years of image analysis. *Nat Methods* **9**, 671-675 (2012).
31. J. L. Veesenmeyer *et al.*, Role of the membrane localization domain of the Pseudomonas aeruginosa effector protein ExoU in cytotoxicity. *Infect Immun* **78**, 3346-3357 (2010).
32. Z. C. Ruhe *et al.*, Programmed Secretion Arrest and Receptor-Triggered Toxin Export during Antibacterial Contact-Dependent Growth Inhibition. *Cell* **175**, 921-933 e914 (2018).
33. Z. C. Ruhe *et al.*, CdiA Effectors Use Modular Receptor-Binding Domains To Recognize Target Bacteria. *MBio* **8** (2017).
34. J. L. Willett, G. C. Gucinski, J. P. Fatherree, D. A. Low, C. S. Hayes, Contact-dependent growth inhibition toxins exploit multiple independent cell-entry pathways. *Proc Natl Acad Sci U S A* **112**, 11341-11346 (2015).